FFI-rapport 2015/02017

Cloud influence on maritime surveillance by an optical satellite

Pål Bjerke

FFI Forsvarets forskningsinstitutt

Cloud influence on maritime surveillance by an optical satellite

Pål Bjerke

Norwegian Defence Research Establishment (FFI)

3 March 2016

FFI-rapport 2015/02017

FFI Project 1318.01

P: ISBN 978-82-464-2692-1
E: ISBN 978-82-464-2693-8

Keywords

Meteorologi

Maritim overvåking

Satellittbilder

Skyer

Approved by

Richard Olsen	Research Manager
Johnny Bardal	Director

English summary

Disturbing clouds may be a showstopper when planning a maritime surveillance satellite with an optical sensor. When the probability of clouds in any place is in the range of 75 %, it is indeed important to know where the clouds are in order to record images as cloud free as possible. The Norwegian Meteorological Institute was contracted to do a study on short term prediction of clouds. The best method turned out to be the interpretation of images from weather satellites taken 2–3 hours earlier. The Norwegian Defence Research Establishment (FFI) was also given access to the cloud information from weather satellites throughout 2014, with only few hours between each observation. These data were used to make statistics to form a basis for evaluating the efficiency of maritime surveillance from a satellite with an optical sensor.

Sammendrag

I planleggingen av en maritim overvåkningssatellitt med optisk sensor er en klar over at forstyrrende skyer er en stor utfordring. Når sannsynligheten for skyer på et gitt sted er ca. 75 %, er det viktig å vite hvor skyene faktisk er for å kunne avbilde de skyfrie områdene. Metrologisk institutt ble engasjert for å se på metoder for skyvarsling. De konkluderte med at den beste metoden var å anta at skyfordelingen var den samme som gitt av dataene fra en værsatellitt 2–3 timer tidligere. FFI fikk også adgang til skyinformasjon i form av tolkede satellittbilder tatt gjennom hele 2014 med få timer mellom hvert bilde. Denne informasjonen ble brukt for å lage statistikk som kunne gi et grunnlag for å vurdere effektiviteten av maritim overvåkning fra satellitt med optisk sensor.

Contents

1 Introduction

FFI is developing new concepts for maritime surveillance with micro-satellites and electro-optical sensors. In many parts of the world, extensive cloud cover represents a serious impediment to efficient image acquisition in the visible part of the electromagnetic spectrum. One approach to achieving better efficiency is to determine cloud-free areas within an area of interest a priori, and task the satellite to image these areas with a shortest possible lead time. This report focuses on issues of cloud cover and cloud prediction. The Norwegian Meteorological Institute (MET Norway) was engaged to help us with the task. They prepared a report on methods to predict clouds and the efficiency of the prediction. A summary of the report is provided in chapter 4, while the report is fully reproduced in appendix A.

Knowing that there are clouds in approximately 75 % of the Norwegian area of interest, an investigation into how the clouds vary in time and space, is of particular interest. By means of cloud information from our near oceans to the west and north of Norway, made available to FFI by MET Norway, it was possible to investigate the distribution of clouds and their movement. The data was analysed for variations through the year, variations through the day, variations through the area and speed of variations. Further on they were used to analyse the influence of clouds on an imaging satellite in a sun synchronous orbit, designed specifically for detection of ships at sea.

This report gives a basis for investigating the efficiency of using optical satellites in cloudy areas, and shows how prediction of the clouds can increase the efficiency.

2 Satellite based optical maritime surveillance

2.1 Operational area of interest

Figure 2.1 Operational area of interest

The main area of interest (AOI), as shown in Figure 2.1, is based on operational interest from Norwegian authorities engaged in maintaining national sovereignty and maritime safeguard and security. The applications include safety at sea, crime at sea and military surveillance. The area spans in the order of 2 million km^2.

Even if the general desire is to control the whole area, parts of the area are more interesting than others, due to locations of fishing grounds and oil/gas extraction. The transit routes for ships in the area are also of interest. Particularly in the case of fisheries monitoring, parts of the area can have a time limited or seasonal interest.

Conceptually, it is also possible to image other parts of the world. However, there would be limitations on the number of images taken due to storage needs in the satellite, time to transfer images from satellite to ground, and necessary battery power to conduct recordings depending on time needed to charge from solar panels.

2.2 Concept for an optical maritime surveillance micro-satellite

FFI has demonstrated space based cooperative maritime surveillance using the Automatic Identification System (AIS). AIS messages are currently intercepted by two nano-satellites, AISSat-1 and -2, currently orbiting the Earth at approximately 600 km altitude in an almost sun-synchronous orbit, i.e. with an orbital inclination of approximately 98° degrees.

Based on the AISSat success, we have started to consider methods for non-cooperative approaches to maritime surveillance, primarily in the Norwegian AOI. One candidate is a micro-satellite mission concept consisting of a small satellite (~50 kg) equipped with an electro-optical (EO) sensor, combined with a VHF radio receiver capable of receiving messages from the Automatic Identification System (AIS).

In the current analysis, we assume that the follow-on AIS-Optical satellite will fly in a similar orbit to AISSat-1 and -2. For the Norwegian AOI, the satellite will pass within the area of interest 6 times during the day, 3 times in the morning and 3 times in the evening, with other passes providing partial coverage of the AOI.

To cover the entire area of interest continuously is a goal that is neither practical nor necessary. Ships travel at low speed compared to other modes of transportation, and voyages often take several days. For example, a ship travelling the length of Norway out at sea covers a distance of more than 1500 km. With a typical speed of 15 knots (27.8 km/h), the journey will take more than 2 days. For the mission concept, we assume that it is sufficient to locate the ship with the optical imager at some intervals, supplemented by AIS on the same platform, as well as other sensors on other platforms.

For the analysis described in the following, we will assume that the satellite can look to each side with a roll-angle of up to 30°, and can image within a swath width of 924 km. Furthermore, we assume that the minimum imaging capacity will be 5 images per pass, and that each image will have a width of 100 km. For simplicity, each image is assumed to be a square of 100 km × 100 km. During a day (30 images), 0.3 million km^2 are covered, and the total area of interest can be covered in 7 days.

For each pass the satellite sees approximately 0.05 mill km^2, or about 10 % of the area of interest. With an average cloud cover of 75 %, a corresponding 25 % of the area will typically be free of clouds. Therefor the satellite can theoretically record completely cloud free areas, assuming it is known where the cloud free areas exist, and that the sensor can point there.

While the main mission concept is to perform wide area maritime surveillance over the entire AOI, It is also possible to scan limited areas of particular interest. Cloud cover statistics can help estimate how efficient monitoring of a certain area would be. For high priority areas, image acquisition can be performed regardless of cloud cover prediction while accepting a higher than desired cloud cover percentage.

Recording other places in the world is fully possible. However, cloud prediction here would be more challenging.

3 Methods for cloud prediction (by MET Norway)

As stated in the previous section, the mission concept involves the use of short term forecasts or nowcasts to estimate a cloud cover distribution for the upcoming satellite pass. We engaged MET Norway to provide an assessment and recommendation on how to provide the best estimate of cloud cover over the AOI over a 6 hour period. Below is a summary of their report which can be found in its entirety in Appendix A.

3.1 Cloud data

Input cloud data for the study were retrieved from a set of images acquired by the following polar orbiting weather satellites: MetOp-A, NOAA-18 and NOAA-19. For study purposes, an area of 1900 km × 1900 km was chosen to work with (Figure 3.1), designed to at least partially match the coverage of the weather satellites, but also very close to the operational area of interest. The images are collected with the third generation Advanced Very High Resolution Radiometer (AVHRR), operating in 6 channels from visible light to thermal infra-red. Each channel of each image consists of 1200 × 1200 pixels, with a pixel size of 1600 m × 1600 m. The weather satellite orbits are designed to be sun-synchronous with an exact repeat cycle of several weeks. This means that the precise coverage varies each day within the repeat cycle. On average, a single image covers about 90 % of the study area.

Figure 3.1 Cloud cover study area

The satellite images were processed using the Polar Platform System (PPS) software developed by the Swedish Meteorological and Hydrological Institute (SMHI), and is used by most meteorological institutes in Europe. PPS transforms the raw data (satellite images) to types of clouds at different altitudes. Comparisons with human synoptic observations show that PPS detects clouds correctly more than 90 % of the time [2]. The false alarm rate (the probability to detect something that is not there), however, is in the range of 5-12 % depending on the time of day that the imagery is collected. This means that PPS over-estimates cloud cover, and that the results in our analysis are somewhat conservative (slightly pessimistic). An example of a satellite image is shown in Figure 3.2 and the corresponding interpreted cloud mask is shown in Figure 3.3.

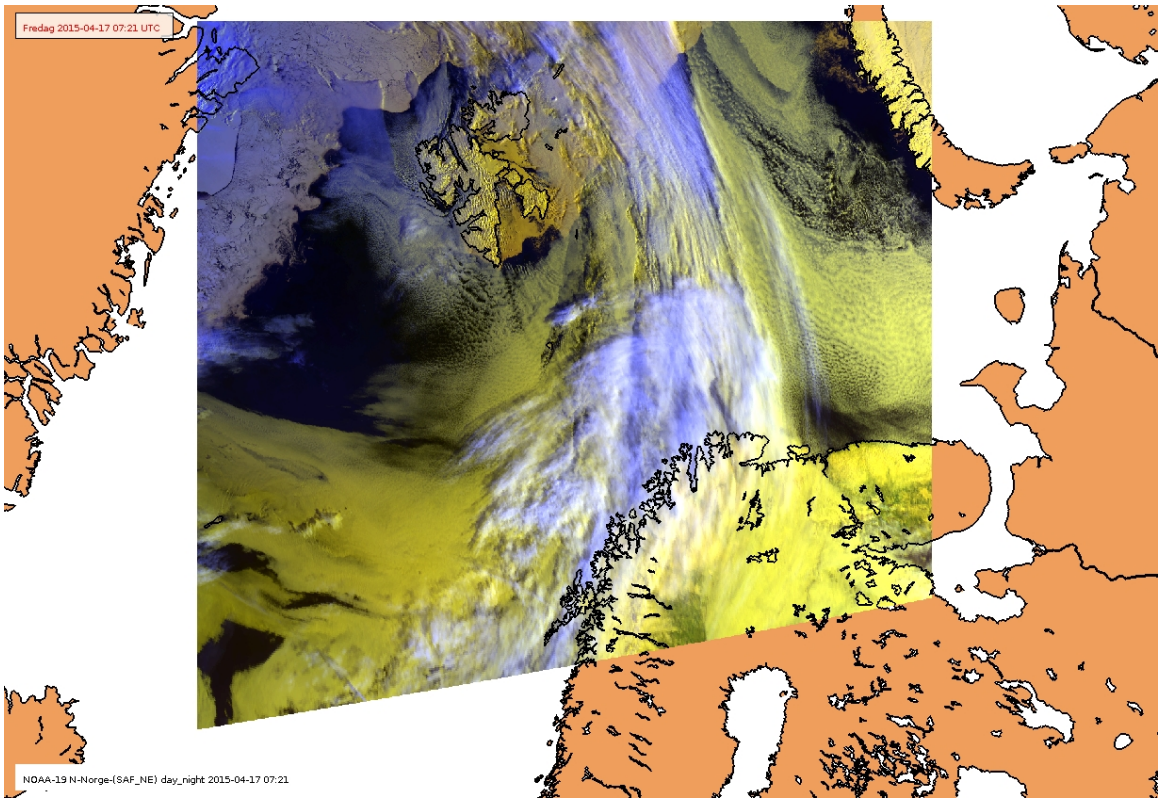

Figure 3.2 NOAA-19 satellite image.

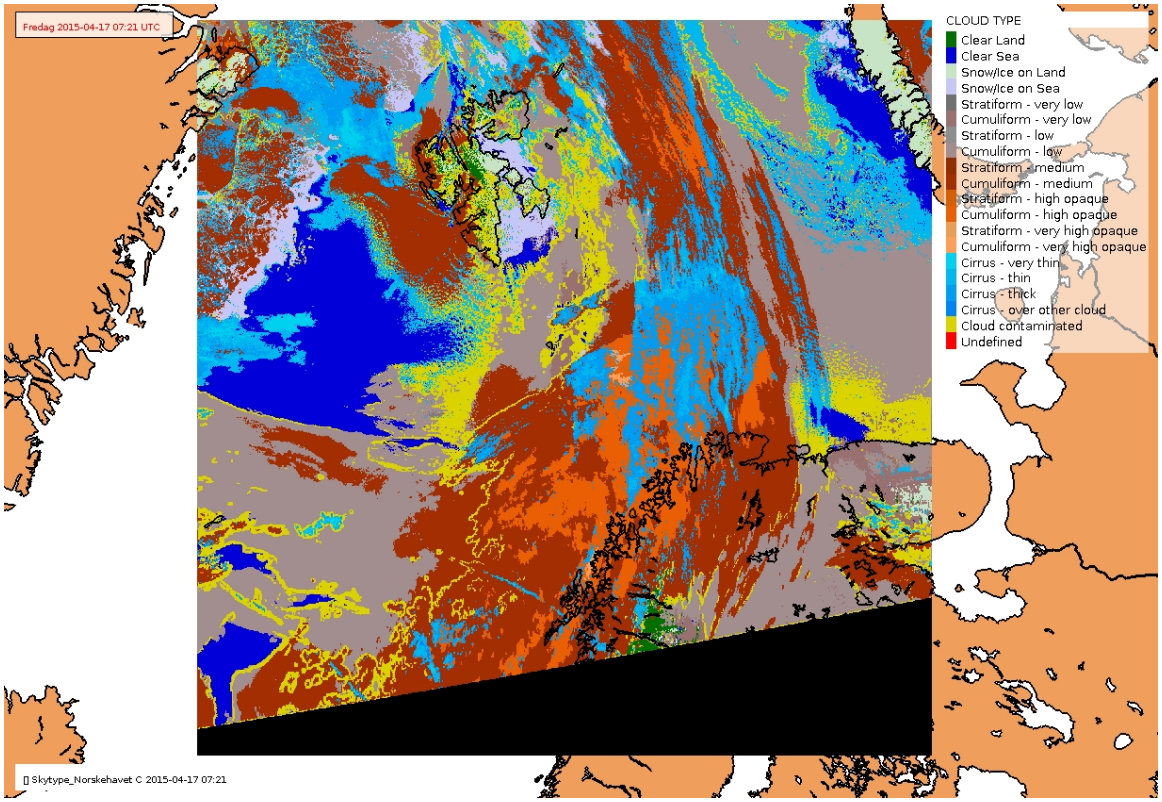

Figure 3.3 PPS cloud classified NOAA-19 image.

The relatively detailed description of the clouds given by PPS is reduced to a simpler grouping more suitable for this investigation, as shown in Table 3.1. The condition “partly cloudy” is a miscellaneous post not completely defined. The condition could occur in continuous areas with clouds almost transparent, or in transitions between overcast and cloud free areas where the pixels could be partly cloudy.

Numerical value	Condition
0	Cloud free (0 % cloud cover)
50	Partly cloudy (50 % cloud cover)
100	Overcast (100 % cloud cover)
255	No data (not covered by recording)

Table 3.1 Coding of clouds

A total of 7348 observations (satellite images) during 2014 were analysed, meaning almost 20 images per day. Since large cloud formations seldom move at high speed, and the pixels are so big (1600 m × 1600 m), the observations can be regarded as almost continuous. This makes the cloud data well suited for an analysis of the AOI.

3.2 Forecast evaluation results

The goal was to evaluate methods of cloud prediction and use the interpreted satellite images as a reference, i.e. the "true" cloud conditions. Prediction intervals were chosen to be 3 and 6 hours. Three prediction methods were considered:

1. Wind field advection: Use the cloud situation at a certain time (time zero), and move the clouds according to an estimated wind field.
2. Numerical Weather Prediction: A weather model (ECMWF- European Center for Medium Weather Forecast) was used to predict the cloud coverage.
3. Persistence: Anticipate that the cloud situation changes very little within the time windows, and just keep the original cloud situation.

To evaluate the methods, we compared the predicted cloud cover with the interpreted satellite image acquired at the forecast time, focusing on methods 1 and 3 above. Figure 3.4 and Figure 3.5 show the average absolute error for each of the methods. A visual inspection shows that the persistence method provides less error than the advection method.

An alternate method for comparison was done by using human observations (SYNOP-Surface SYNOPtic observations) as a reference. These observations were from 3 ocean stations and 7 coastal stations. By comparing average absolute error, the 3 hour persistence method was the best estimate. Use of advection and weather model was however better than the 6 hour persistence. The results are shown in Figure 3.6.

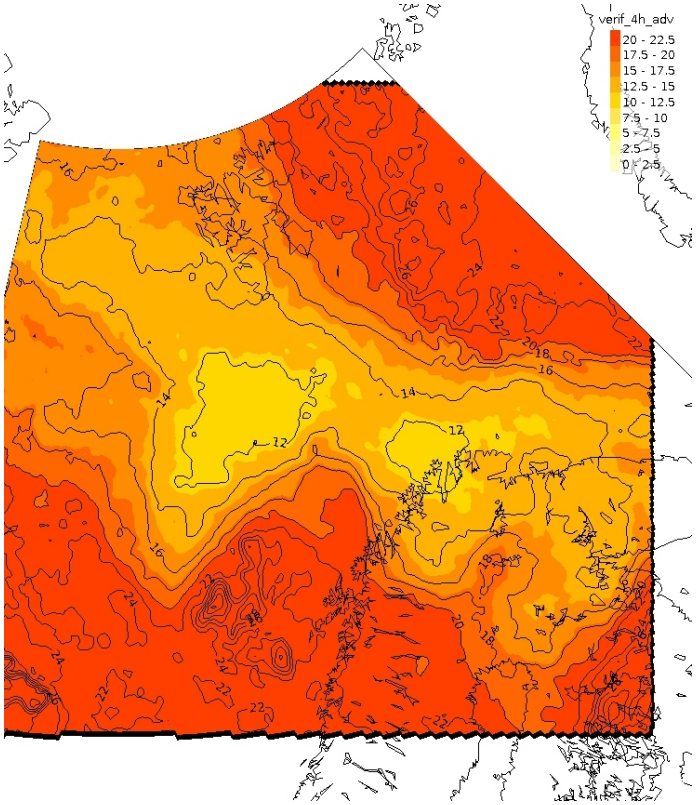

Figure 3.4 Average absolute error of cloud prediction based on advection.

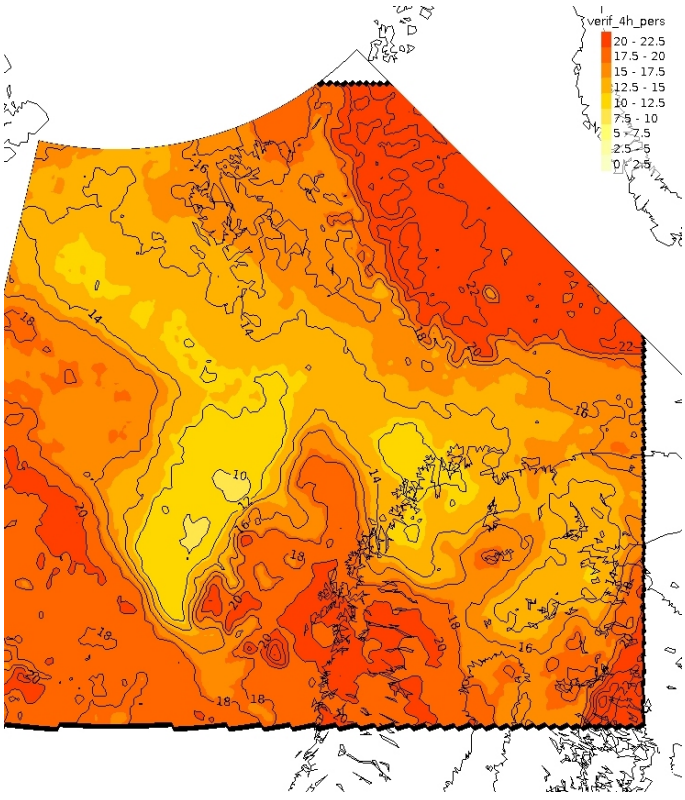

Figure 3.5 Average absolute error of cloud prediction based on persistence

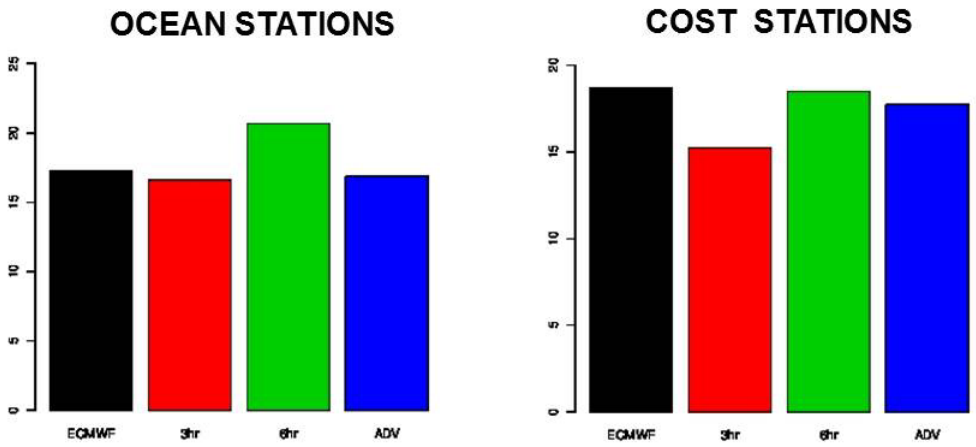

Figure 3.6 Comparing average absolute error for the methods of prediction using SYNOP registrations from the ocean- and coast stations.

4 Analysis of cloud coverage

FFI got access to cloud data for the area of interest for 2014 from the MET Norway. The purpose was to study how clouds would obstruct optical satellite images of the ocean. By looking at the ways clouds are spread in space and time, it is possible to obtain knowledge of how effective the surveillance will be. It is of particular interest to see if certain regions or periods of time had increased cloud coverage. By analysing the cloud data, a statistical basis was provided for evaluating satellite based maritime surveillance using optical sensors.

Apart from the statistical analysis of cloud conditions, a more realistic simulation with simulated satellite orbits is conducted. The efficiency of the recordings is based on how cloud free the images are. An important part of the concept is the prediction of clouds based on data from weather satellites, giving us the opportunity to point the satellite at the most cloud free areas in its passes.

4.1 Yearly average

The different cloud conditions for every pixel on every day of the period are summed up for the area of interest (oceans only), yielding the percentage given in Table 4.1.

CLOUD CONDITION	PERCENTAGE PART
Cloud free	18,2 %
Partly cloudy (50 % cloud cover)	9,2 %
Overcast (100 % cloud cover)	72,6 %

Table 4.1 Cloud conditions for the area of interest.

The result offers a negative perception of the possibilities for the using of optical sensors in the area of interest. These numbers, however, do not give any information on the variation in time and space. Neither do they tell how fast the cloud conditions are changing. Figure 4.1 shows the distribution of observations (satellite images) as a function of cloud free percentage. The plot shows that the level of cloud free existence is concentrated in the range of 10-40 %. None of these images were more than 60 % cloud free.

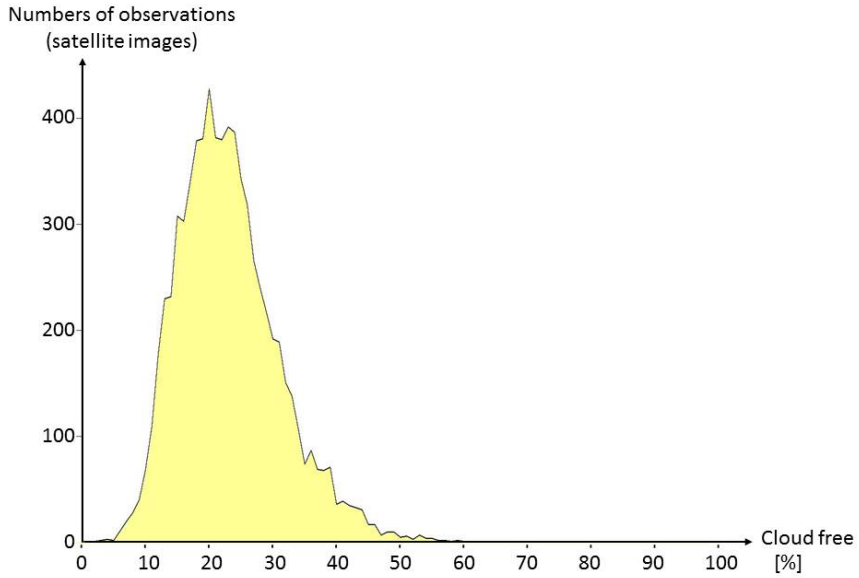

Figure 4.1 Distribution of observations (satellite images) as a function of cloud free percentage.

4.2 Yearly variation

It is important to know in which way the cloud conditions vary throughout the year, and eventually influence the possibility to image efficiently through certain periods of the year.

Figure 4.2 shows how the cloud free conditions vary through the year for the the total area of interest (pixelwise). For each day of the year we have accumulated the cloud free condition over shorter periods of time, for 1day (blue plot), 3 days (green plot) and 5 days (violet plot). The curves show clearly how the cloud free part of the area increases as the time of accumulation increases. This is simple evidence of the continuous movement of the clouds. In Table 4.2 the minimum and average values of the curves of Figure 4.2 are tabulated.

The cloud free condition throughout the year is rather stable with larger changes from day to day. The positive experience with these results is the rather rapid movement of the clouds showing an average cloud free condition of 62,7% accumulated for 1 day, opposed to 18,2% for the general average.

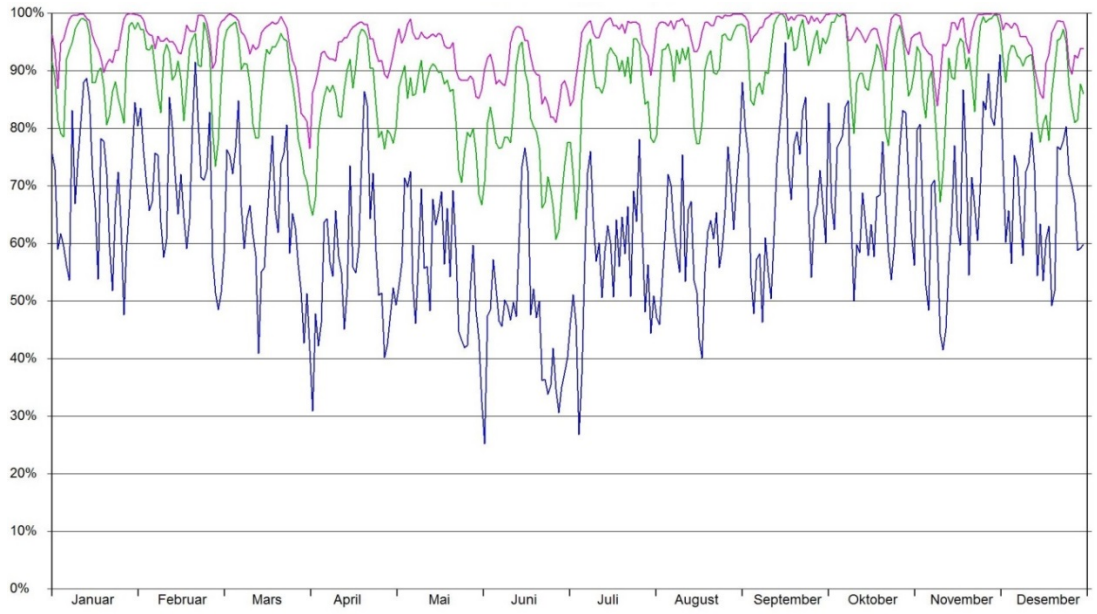

Figure 4.2 Available cloud free conditions accumulated for 1 day (blue plot), 3 days (green plot) and 5 days (violet plot).

No of days accumulated	Minimum cloud free area [%]	Available cloud free area [%]	Plot colour
1	25,2	62,7	Blue
3	60,4	88,1	Green
5	77,2	95,3	Violet

Table 4.2 Accumulated cloud free conditions for the total area of interest (sea part)

4.3 Daily variation

Imaging satellites often move in sun synchronous orbits. This means that the satellites use orbits in which each satellite passes the same positions on the earth at the same time of the day. This is especially attractive for optical imaging satellites since the light conditions in a certain spot will be the same for each pass. During a day the satellite will pass the same spot 3 times, going upwards (south to north), and 3 times going downwards (north to south). The passes will typically take place in daytime and in the evening. Due to this fact, it is important to investigate the cloud variations throughout the day, i.e. the daily variations in cloud cover.

The cloud data from 2014 had a time distribution (GMT) of observations (weather satellite images) shown in Figure 4.3. The distribution is related to the choice of weather satellites and their orbits. The data had no observations between 21:00 and 00:00. Apart from this, the images were relatively evenly distributed throughout the day with a concentration at mid-day and a more sparse distribution against the evening and morning.

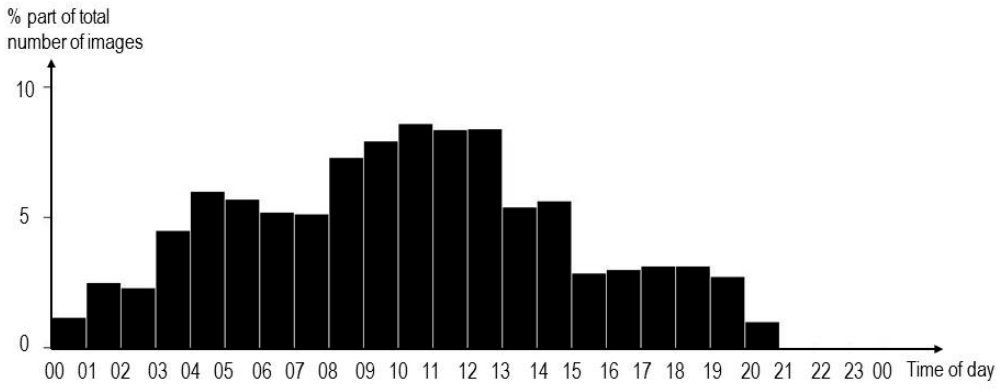

Figure 4.3 Distribution of number of cloud observations (satellite images) throughout the day (GMT).

The result of the daily cloud cover analysis is shown in Figure 4.4. The bars show the average number of observations through the day for the the 3 different cloud conditions; cloud free (blue bars), 50% cloud coverage (light blue bars) and overcast (grey bars). The figure shows how stable the cloud condition is throughout the day. There is, however, seemingly a small trend showing less cloud free conditions in the daytime corresponding to an increased portion of 50 % cloud coverage. However, this could be due to measurement inaccuracy since observations in the night are based on thermal infrared images which can have problems with the contrast between clouds and the ocean (the background). The overcast part is almost constant.

The result shows that the cloud conditions will be almost independent of the time of the day, which is of importance in connection with planning satellite orbits.

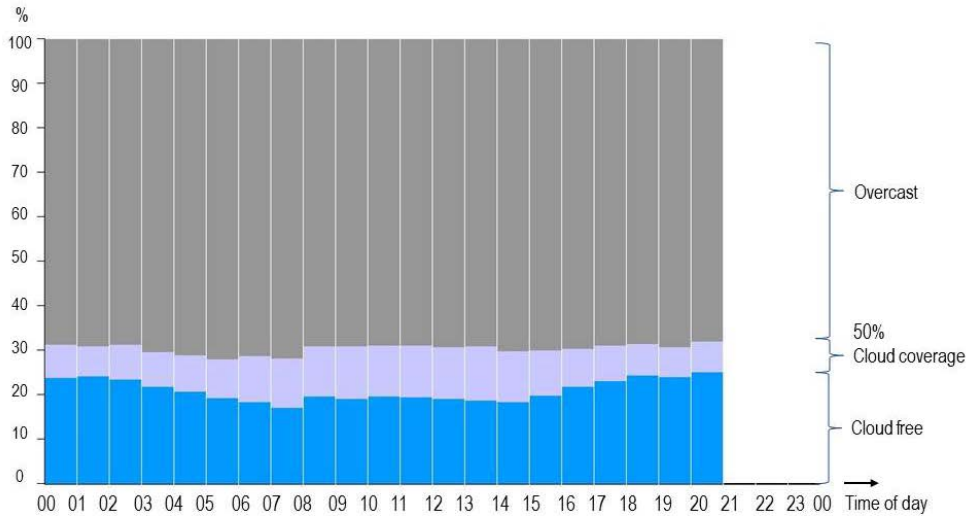

Figure 4.4 Distribution of average cloud condition through a day (2014). Blue bars: Cloud free conditions, Light blue bars: 50% cloud coverage and Grey bars: Overcast.

4.4 Spatial variation

The area of interest is so large that it is fair to believe that the cloud conditions will vary as a function of position. For example the cloud conditions close to land are expected to be different from the cloud conditions on the open ocean. The wind patterns on the ocean most probably influence the amount of clouds as well as their shapes.

The top image in Figure 4.5 shows the average cloud free area throughout 2014 as function of geographical position. A region in the Norwegian Sea south and west of Svalbard as well as the region towards Novaya Zemlya (red colour in Figure 4.5), has a higher concentration of clouds than the rest of the area of interest. Here only 5-10 % of the area is cloud free. The pattern is not very different from the way the Gulfstream moves. Typically the coast areas are more cloud free than the open ocean, being more than 20 % cloud free. The corresponding numerical values are shown in Table 4.3.

The lower image in Figure 4.5 shows the average cloud coverage, but it also includes the ship activity in the same period of time, visualized by white spots. The ship activity is made from AIS data from 2014, and every white spot represent ship activity over some limit. The limit is based on statistics and is given by the probability for the presence of a ship is greater than 3 %.

The majority of shipping activity in this region is connected to fishery. Those are commonly found in the fishing areas in the ocean between Norway and Svalbard. From the overview image in the lower part of Figure 4.5, these areas are unfortunately mainly found to coincide with the cloudiest areas.

Colour	Cloud free	Part of area of interest
	0-5 %	0,0 %
Red	5-10 %	23,1 %
Orange	10-15 %	32,5 %
Yellow	15-20 %	17,1 %
Yellow Green	20-25 %	18,0 %
Green	25-30 %	6,7 %
Dark green	>35 %	2,5 %

Table 4.3 Distribution of cloud free levels relative to percentage part of area of interest.

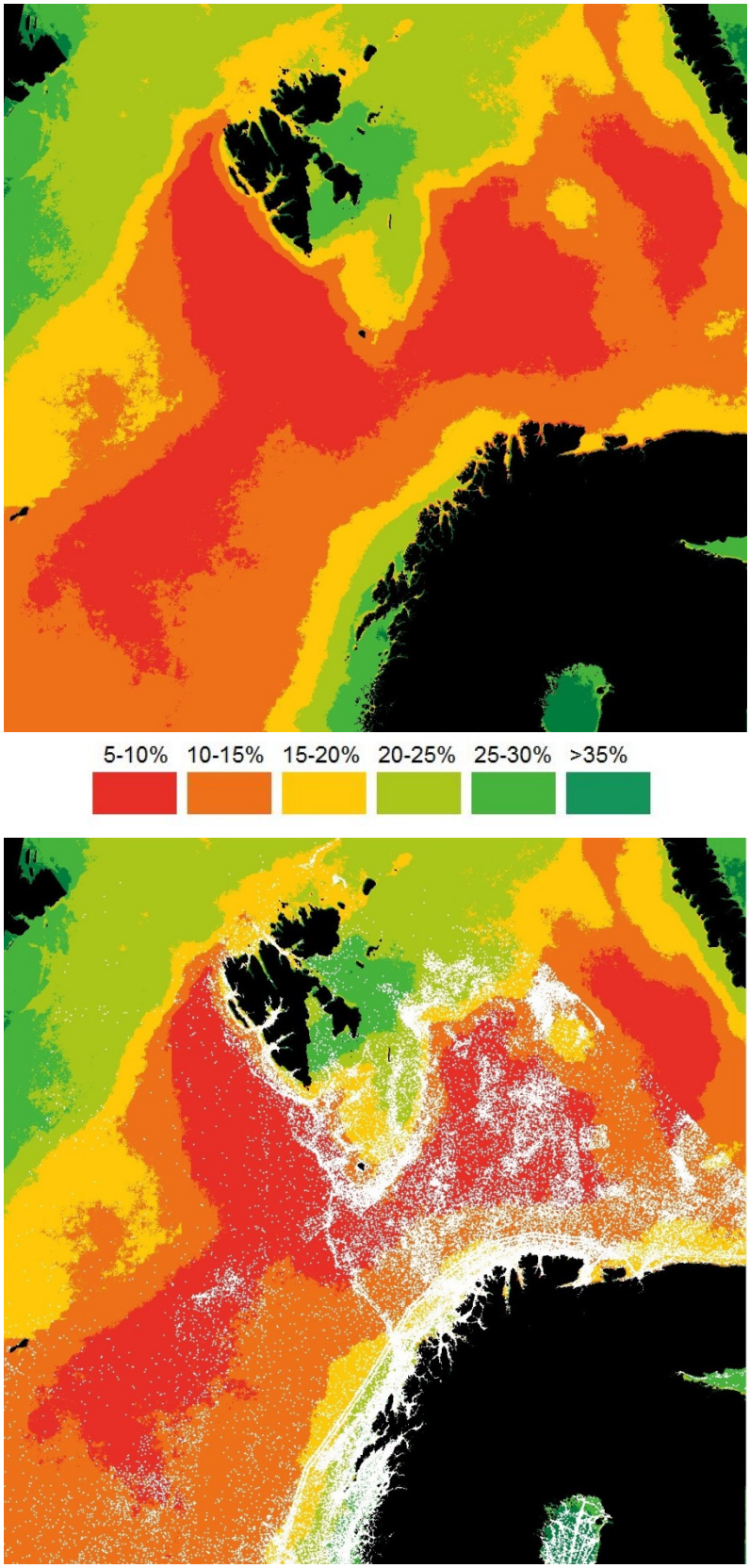

Figure 4.5 Regions with different levels of cloud free average through 2014. Lower image is similar to the top image but has included ship activity in the same time period (AIS data).

4.5 Rate of change

Efficient optical surveillance is dependent on areas not being covered by clouds for long periods at the time. From the cloud data from 2014 the maximum number of days with continuous overcast for each position (pixel) was calculated. The area to be analysed had to have coverage for every observation through the year, for the results to be correct. The limited area satisfying this request is shown in Figure 4.6 displaying the results of the survey. Calculated numbers are shown in Table 4.4, which also provides the colour coding used in Figure 4.6.

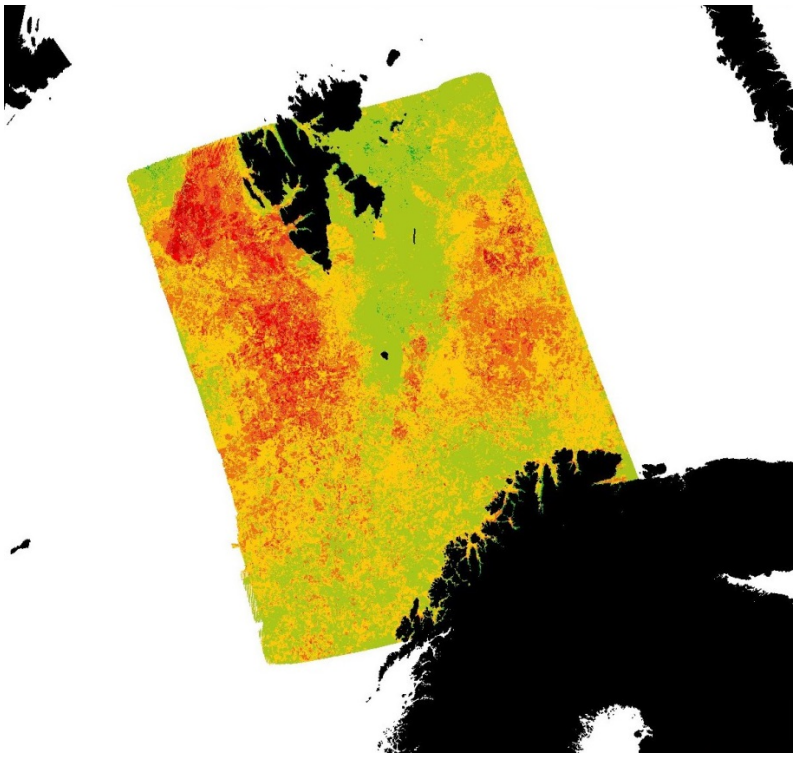

Figure 4.6 Maximum number of days with continuous clouds. Colour coding as shown in Table 4-3

Table 4.4 shows the maximum time with continuously overcast and their percentage part of the total area as the worst case condition. The longest continues overcast for a position was measured to be 41 days. The average maximum continues overcast for the total area of interest, however, is only 1.3 days.

Colour	Maximum number of days continues overcast	Part of Area [%]
Green	0-3	5.8
Yellow Green	4-7	37.9
Yellow	8-11	34.2
Orange	12-15	15.7
Red	16-19	4.4
Dark red	>19	0.9

Table 4.4 Maximum number of days with continues overcast

5 Analysing the influence of cloud cover for the use of satellite images

The analysis in chapter 4 covers in general statistical cloud conditions in the area of interest. The motivation for this report is, however, the influence of clouds on satellite images. This chapter will address the combination of statistical cloud conditions and the use of optical imaging satellites. It is of interest to evaluate the efficiency (level of cloud free recordings) for the orbits of the satellite with regard to the time of the passes and the area covered.

We will assume a satellite orbit as described in chapter 2.2 with a capacity to record 5 images per pass and doing 6 passes per day. Each image covers 100 km x 100 km, and the satellite can point up to 30° to each side.

5.1 Daily imaging with no limitations in space and time

The satellite can record 5 images in each of its 6 passes per day, all together 30 images a day. As a reference for the efficiency of recordings (the amount of cloud free conditions in the recordings) from satellite passes, we found the 30 most cloud free recordings for each day of the year without limitations concerning recording time and area dictated by satellite orbits. It was assumed that the cloud conditions were known from predictions (weather satellite images). The results were listed according to the level of cloud free conditions. The cloud data consists of 7348 observations (interpreted satellite images) and the search was both comprehensive and time consuming. The result from each observation was registered and visualised in an image as the example in Figure 5.1 shows. Clouds are shown as white regions while cloud free areas are shown as blue regions. In addition it is shown red frames indicating potential satellite images ranged after the level of cloud free condition and marked with a number telling the cloud free percentage.

The result in Figure 5.2 shows each day of the year represented as a vertical bar. The colour coding shows the level of cloud free condition for each of the daily 30 recordings. Almost every day has a number of totally cloud free images. For some days the least cloud free images contains more than 50 % clouds. The distribution of cloud free images through the year is shown in Figure 5.3. It was calculated that the average efficient use (amount of cloud free conditions) for the year is totally 95.8 %.

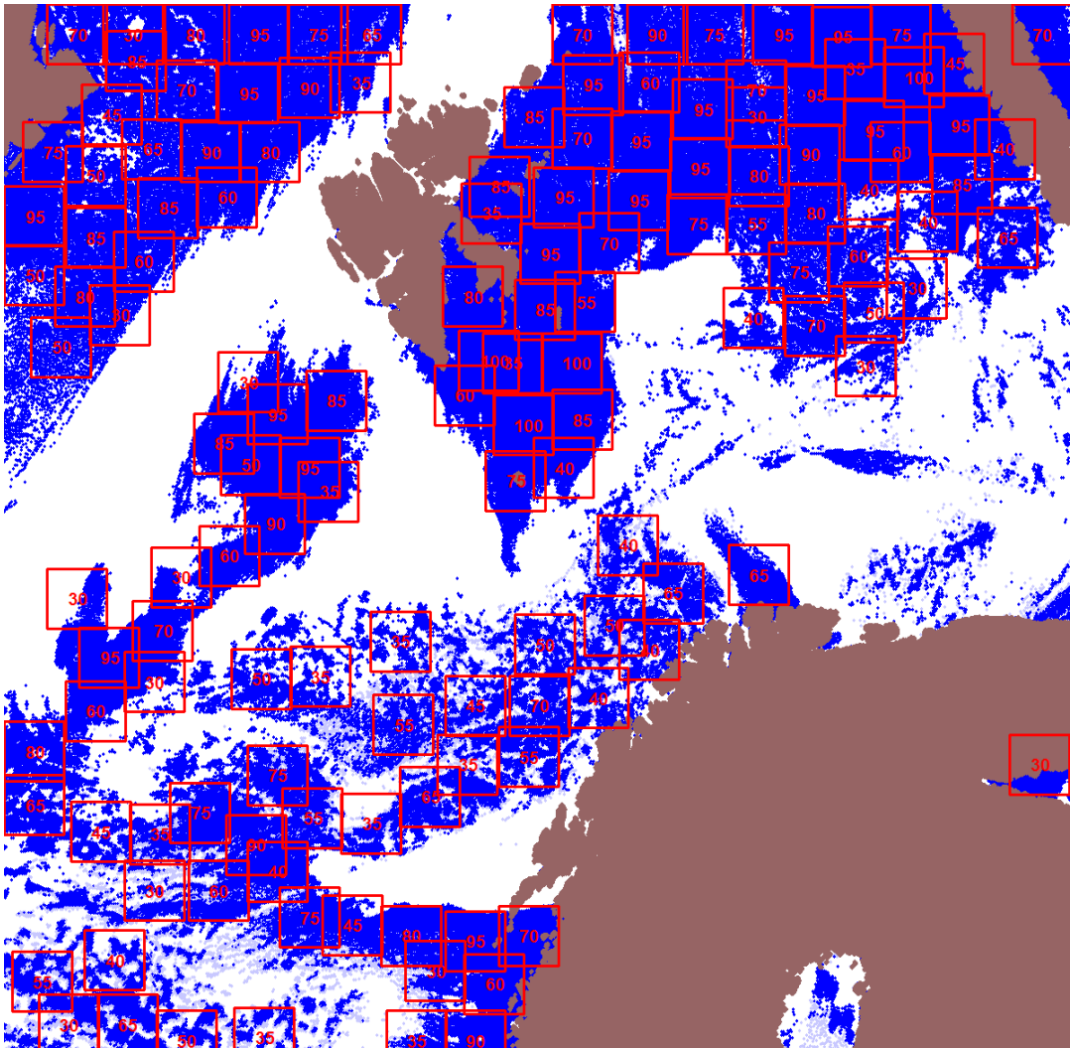

Figure 5.1 Example of potential satellite images in cloud free areas

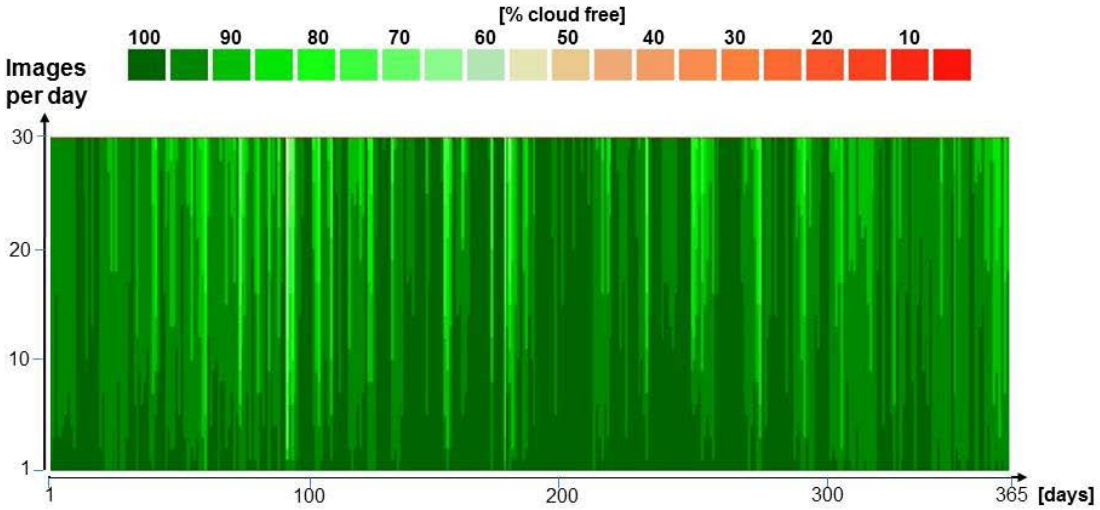

Figure 5.2 The 30 daily most cloud free images per day throughout a year. No restrictions in time or space. The level of cloud free condition is colour coded as indicated on the top.

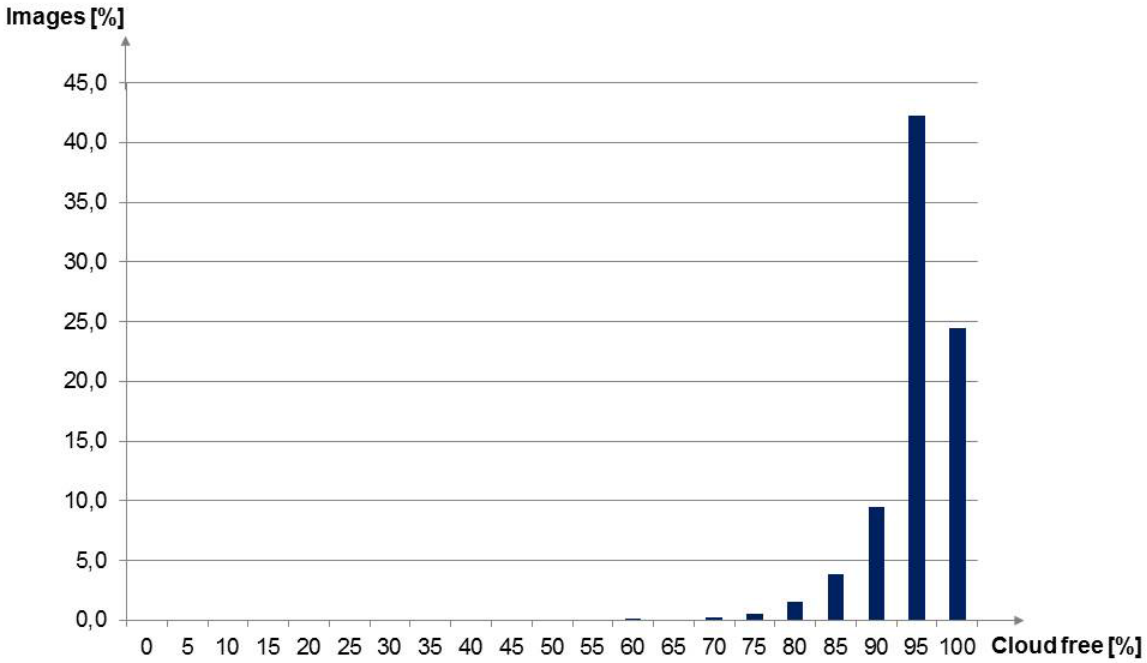

Figure 5.3 Distribution of the 30 daily most cloud free images throughout a year ranked after the level of cloud free condition. No restrictions in time or space. The horizontal axis shows the average level of cloud free conditions. The vertical axis shows the procentage number of the images.

Earlier it was found how the cloud condition varies over the area of interest. Figure 5.4 shows the 30 most cloud free images per day accumulated over each month of the year. It shows that the cloud free areas are concentrated, and cover the same regions several times while others are uncovered. The number of images recorded through a month (840 – 930 images) covering a total an area 2-3 times larger than the area of interest.

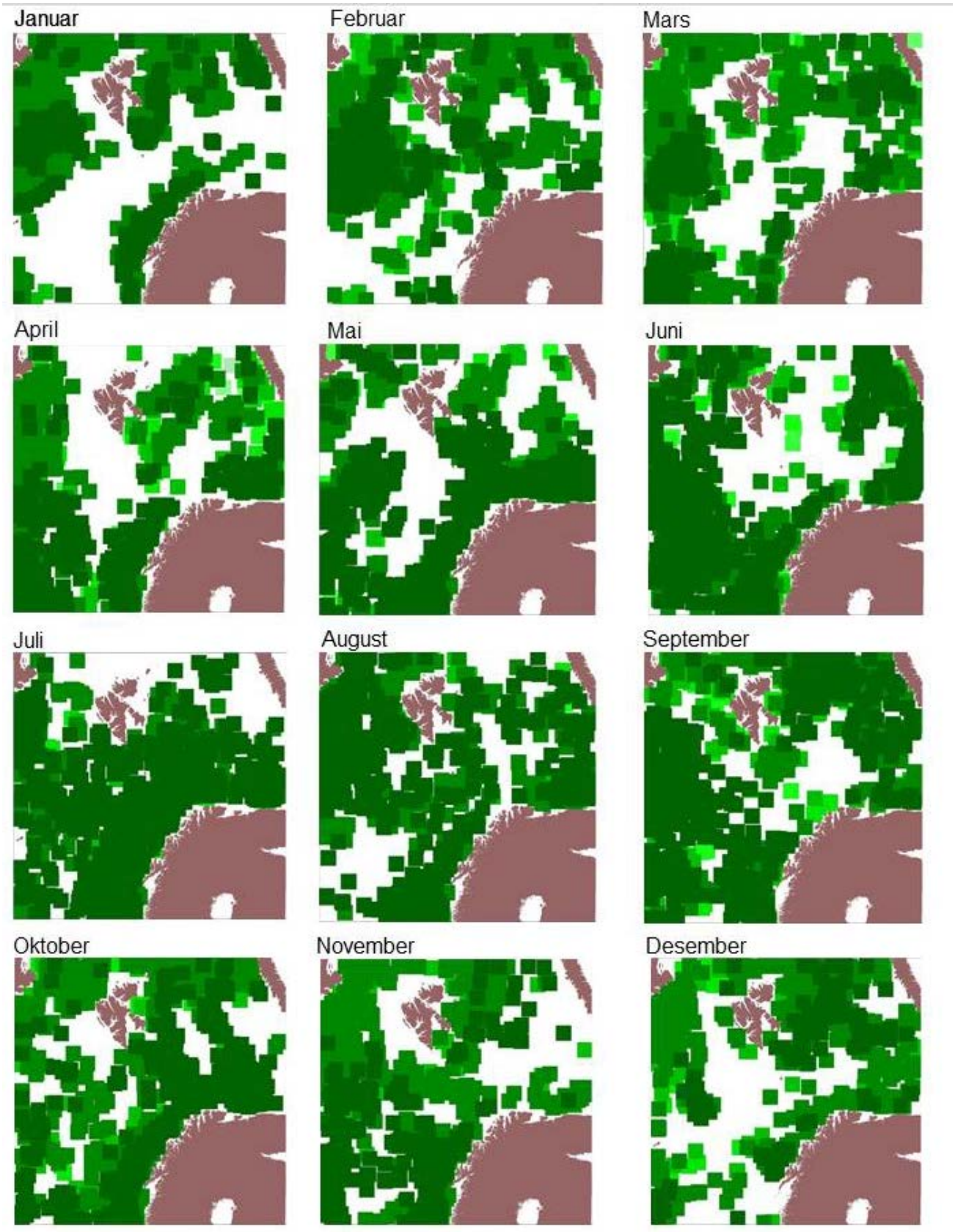

Figure 5.4 Monthly cover of the 30 most cloud free images per day with no restrictions.Efficiency (cloud free part of images): 95.8 %.The same colour coding as in Figure 5.2.

5.2 Daily imaging restricted by simulated satellite passes

The ultimate test is to combine the cloud conditions through the year with realistic coverage from satellite. The satellite orbits for the AIS satellites were used as examples, and consequently an orbit altitude of 600 km and an inclination of 98° were chosen. Since the satellite is able to point 30° to each side, this gives a width of coverage of 924 km. The satellite covers the area of interest several times a day, but only 3 passes in the morning and 3 passes in the evening will have the orbit over the complete area of interest. To simplify the calculations, the satellite orbits were modified to cover a simpler geometry, as shown in Figure 5.5. Since the orbit will be a little displaced every day in a cycle of 12 days (revisit time), the average time of the passes were used as shown in Table 5.1.

Direction of pass	Time of day		
North to south	11:30	13:00	14:30
South to north	18:30	20:00	21:30

Table 5.1 Time of passes for a simulated imaging satellite

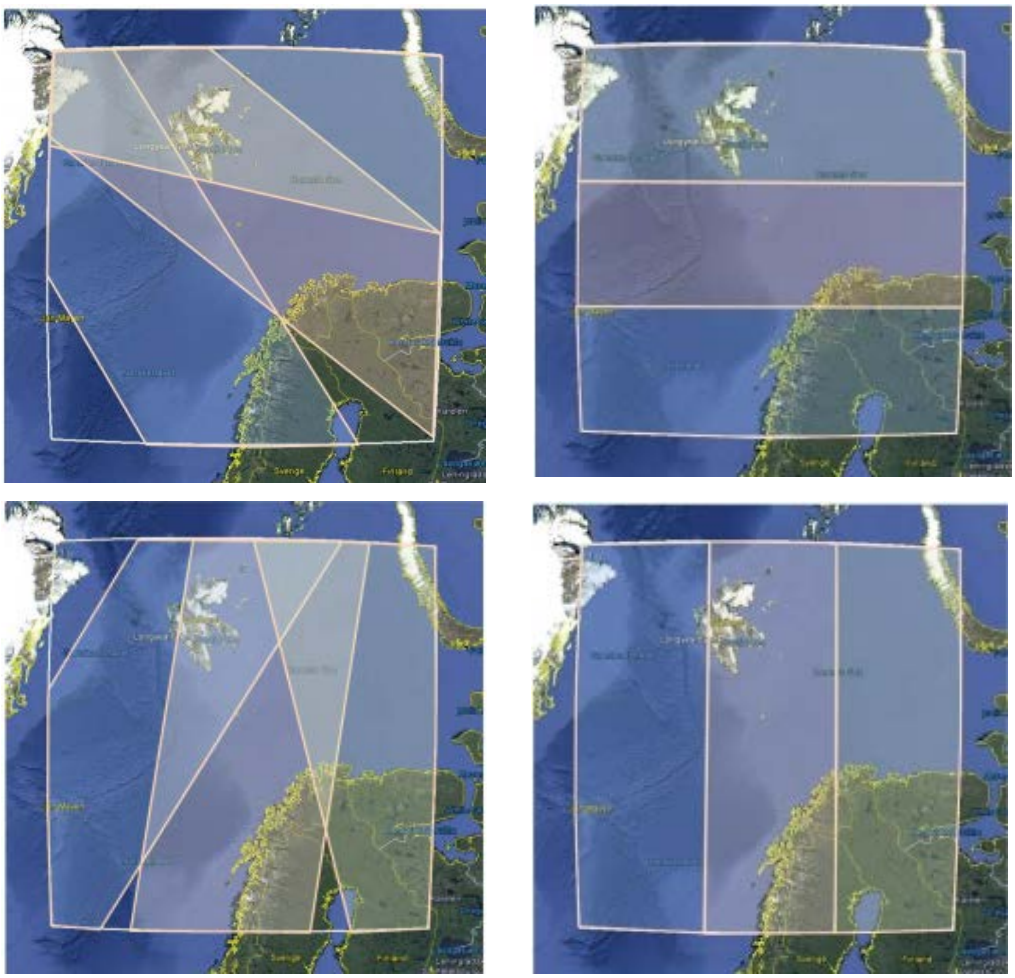

Figure 5.5 Simplified satellite orbits. Left: Coverage from actual orbits Right: Coverage from simplified orbits Top: South to north (evening) Bottom: North to south (morning).

The search for the most cloud free images was then limited to the satellite passes over the area of interest. The results are shown in Figure 5.6 and Figure 5.7, and are to be compared to the results in Figure 5.2 and Figure 5.3. The limitations implied by following the satellite orbits, clearly result in less cloud free recordings. Almost daily the recordings show less than 50 % cloud free conditions, showing an orange/red colour in Figure 5.6. For some days it is not even possible to find 30 images that do not contain one or more overcast recordings. The average cloud free condition through the year was calculated to 68.1 %.

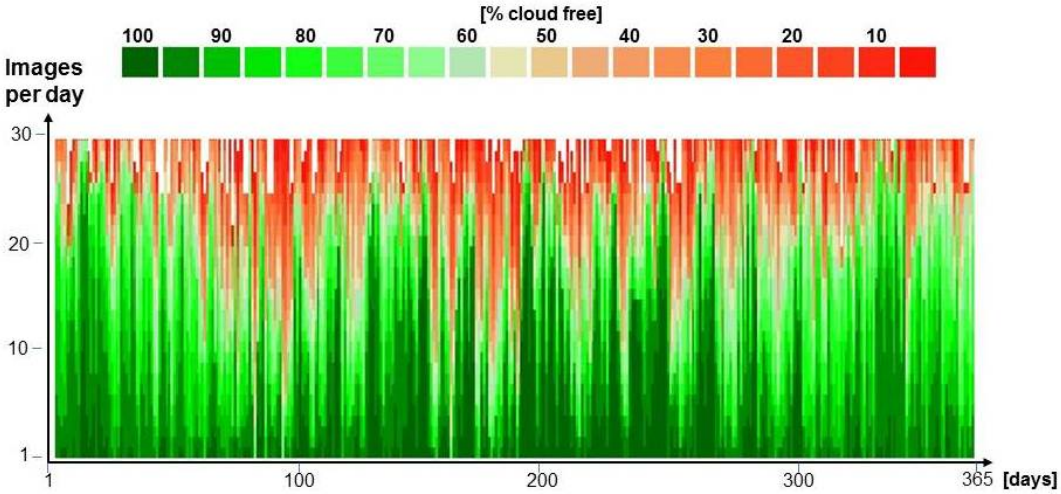

Figure 5.6 The 30 daily most cloud free images per day throughout a year. Restricted to simulated satellite passes. The level of cloud free condition is colour coded as indicated on the top.

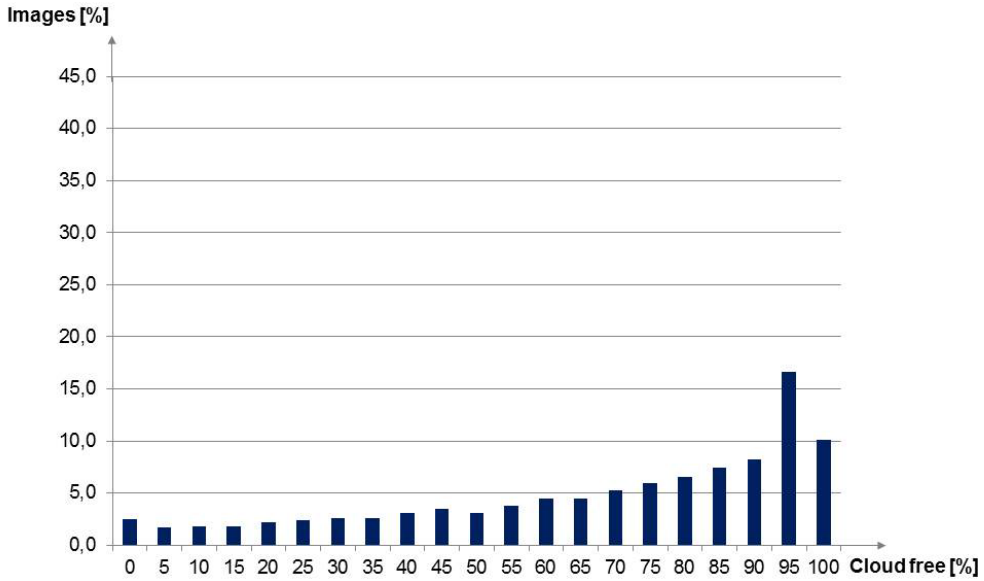

Figure 5.7 Distribution of the 30 daily most cloud free images throughout a year ranked after the level of cloud free condition. The images are restricted to simulated satellite passes. The horizontal axis shows the average level of cloud free conditions. The vertical axis shows the procentage number of the images.

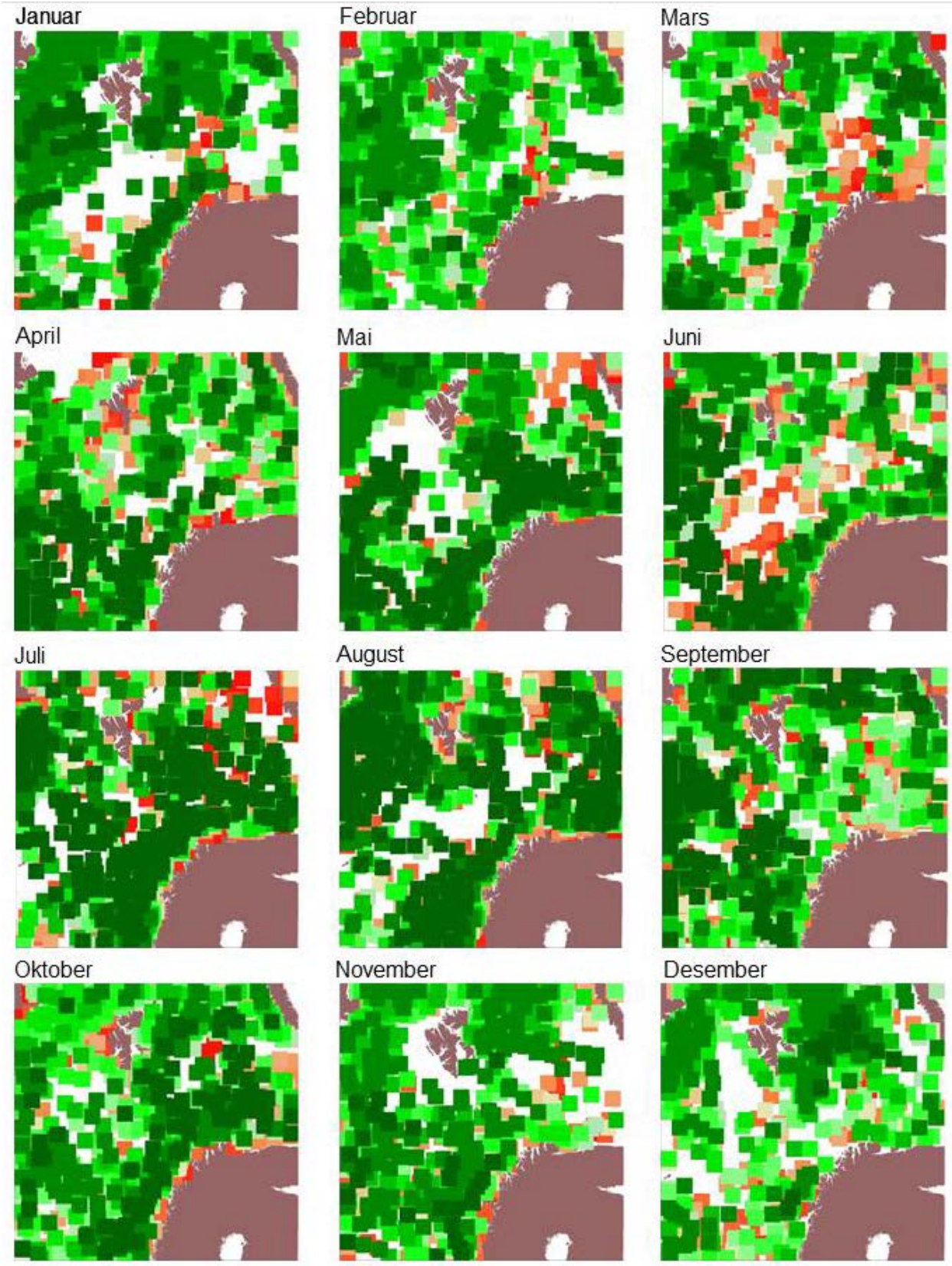

Figure 5.8 Monthly coverage of the 30 most cloud free images per day limited by simulated satellite orbits. Efficiency (cloud free part of the images): 68.1 %.Colour coding as in Figure 5.6.

Figure 5.8 shows the 30 most cloud free images per day accumulated over each month of the year restricted to the simulated satellite orbits. Compared with Figure 5.4, where the images are without limitations, the difference is clear. The efficiency (amount of cloud free conditions) has fallen from 95.8 % to 68.1 %. The green colours in Figure 5.4 indicating (almost) cloud free images, have been partly substituted with red/orange colours indicating less cloud free areas in Figure 5.8

6 Summary

This report shows how clouds influence maritime surveillance using a satellite based optical sensor. Cloud data from 2014 for the area of interest, the oceans west and north of Norway, have been statistically analysed.

The average cloud free conditions throughout the year for the area of interest is measured to be 18.2 %, which is the starting point for the efficiency of recording from satellite with an optical sensor.

The variations through the year have a fairly steady average with large variations locally in time. A slight trend showed less cloud free conditions in the summer. Accumulating data over time results in increasingly available cloud free images. Accumulating for only one day (24 hours) results in that the cloud free conditions increases to 62.7%.

Vaariations throughout the day were negligible, except for a possible slight trend showing less cloud in the nights.

The spatial variation is distinct and shows on average more clouds in regions of the open sea, and more cloud free conditions closer to land. Some regions of the sea appear to be particularly cloudy, with the average cloud free conditions below 10%.

The rate of change of cloud conditions varies throughout the area of interest. Average maximum duration of overcast in a position is 1.3 days, while the highest value is staggering 41 days.

Based on an imaging satellite obtaining images of the size of 100 km x 100 km, and a capacity of 30 images per day, the efficiency (amount of cloud free conditions) was calculated from simulations using cloud data from 2014. The cloud conditions were assumed known through observations (interpreted satellite images). The most cloud free images were searched for with no limitations to space and time. The efficiency was found to be 95.8 %.

A similar simulation as above was conducted, also taking simulated orbits into account. Using almost the same satellite orbits as the AIS satellites, the most cloud free images were searched for each day limited in space and time according to the satellite orbit. The efficiency was then found to be 68.1 %.

7 Conclusion

Clouds limit the efficiency of using optical imaging satellites for maritime surveillance. In our area of interest there will be on average 18.2 % chance for cloud free conditions throughout the year. Since the cloud situation constantly is changing, cloudy regions will over time become cloud free. Only after 24 hours the accumulated average cloud free conditions is raised to 62.7%. Available weather satellites can predict cloud conditions in near real time, giving us the necessary information to predict cloud free areas and aim there in an automatic way. With a capacity of 30 images per day, 5 images in each of 6 orbital passes, the efficiency (the cloud free part of the images) will be increased to 68.1%.

The increased efficiency obtained by predicting cloud conditions, make optical satellites a good candidate for maritime surveillance.

Vedlegg A Report from MET Norway

Description and verification of Cloud forecasts with short lead times in maritime areas.

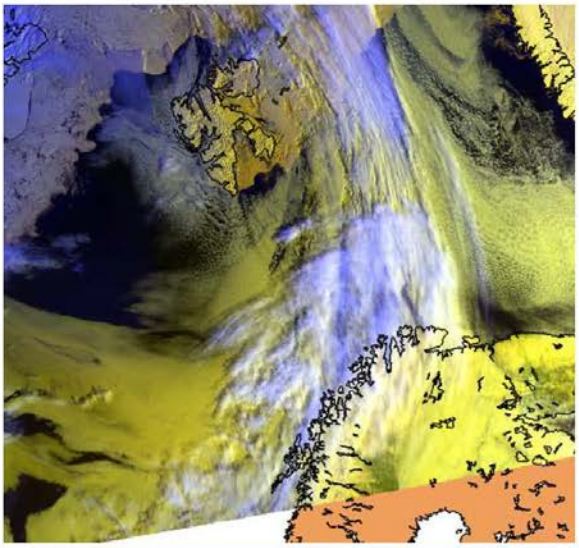

Morten Køltzow, Atle Macdonald Sørensen, Frank Tveter and Steinar Eastwood.

Meteorologisk institutt

1

1. Introduction

This report describes the results from the project "Utvikling av maritimt skymaske-produkt", a co-operation between Norwegian Meteorological Institute (MET-Norway) and Forsvarets Forsknings Institutt (FFI).

The objective of the project was to evaluate cloud forecast products available at MET-Norway for Norwegian ocean areas in the context of now-casting with a lead time of 2 to 4hr. In addition, a new cloud forecast product based on advection of a satellite-based cloud mask was developed and tested.

Two independent observation types for cloud cover are described and compared in chapter 2, namely the satellite-based cloud mask product and SYNOP-observations. In chapter 3, we give a description of the available cloud forecasts. This is the output of the Numerical Weather Prediction (NWP) model ECMWF, persistence and advection of the cloud mask product. The description of the advection of the cloud mask is done in more detail as the forecast product is developed with in the project. In chapter 4 we describe the Norwegian cloud climatology based on Synop-observations. Further, we compare forecast products based on the cloud mask with the cloud mask itself in chapter 5, while all forecasts are verified against independent SYNOP-observations in chapter 6. In chapter 7 we summarize the results.

2. Observation

2.1 Satellite based cloud mask

The AVHRR (Advanced Very High Resolution Radiometer) satellite instrument measures the incoming radiation in specific spectral bands in the visible and infrared spectrum. The data is then processed using the PPS (Polar Platform System) package [1] to convert the raw data to cloud products including Cloud Type and Cloud Mask.

We use data from three of these instruments, namely those flying on the MetOp-A (or MetOp-02 as it's designated in our filenames), NOAA-18 and NOAA-19 satellites. These are all polar-orbiting satellites that are currently in orbit and sending us data.

This PPS cloud type product, which is the one we use as the truth value at the starting time for the advection process described in chapter 3, classifies each cell in the target area as one of the cloud types given in table 1 below.

Now, these files are available to us as HDF files, so our very first step in the cloud advection process is to convert these to NetCDF files (NetCDF4). During this conversion we keep the cloud type variable and associated quality flag and also introduce a cloud cover variable which is merely the cloud type converted to a cloud cover percentage for each grid cell. When creating this cloud cover we use the conversion given in table 2.

Using a Fill_Value for cloud type 0 and 20 in table 2 assures that undefined cloud type cells lead to corresponding undefined cloud cover cells. PARTIAL_CLOUD has a default value of 50% that is the one we've used during processing.

We also add a cloud forecast variable which will hold the results from the cloud advection after we have run the process. This variable will contain the cloud cover prediction for the first six full hours

after the satellite time. At this stage each time step has a dummy value which is mostly a copy of the cloud cover variable.

ID	Cloud Type	ID	Cloud Type
0	Not processed	11	High and opaque cumiliform cloud
1	Cloud free land	12	High and opaque stratiform cloud
2	Cloud free sea	13	Very high and opaque cumiliform cloud
3	Snow/ice contaminated land	14	Very high and opaque stratiform cloud
4	Snow/ice contaminated sea	15	Very thin cirrus cloud
5	Very low cumiliform cloud	16	Thin cirrus cloud
6	Very low stratiform cloud	17	Thick cirrus cloud
7	Low cumiliform cloud	18	Cirrus above low or medium level cloud
8	Low stratiform cloud	19	Fractional or sub-pixel cloud
9	Medium level cumiliform cloud	20	Undefined
10	Medium level stratiform cloud		

Table 1: Cloud type classification from PPS.

Cloud Type	Cloud Cover
0, 20	Fill_Value
[1,4]	0%
[5,18]	100%
19	PARTIAL_CLOUD

Table 2: Conversion used when creating cloud cover variable.

The resulting filenames are on the form:
{satellite}_{date}_{time}_{orbitnumber}.{area}.{variable}_{coverage}.nc

where coverage is a number from 000 to 100 representing the fraction of the product area for which we have cloud data (i.e. metop02_20140606_0855_39590.dnnr.cloudtype_097.nc). The other parts of the filename should be clear including the orbit number which is a satellite-specific number that is incremented for each orbital revolution around the earth.

In Figure 1 and 2, we show the product area with the raw satellite data and the resulting cloud type classification, respectively. In the following we use the short-name CM for the cloud mask product.

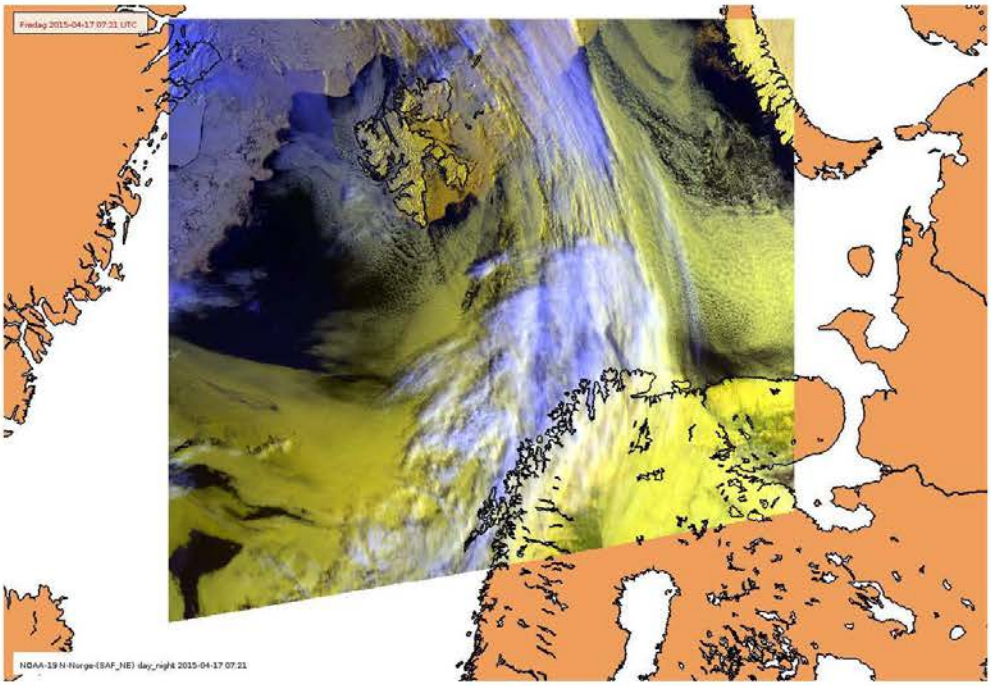

Figure 1 NOAA-19 day_night image.

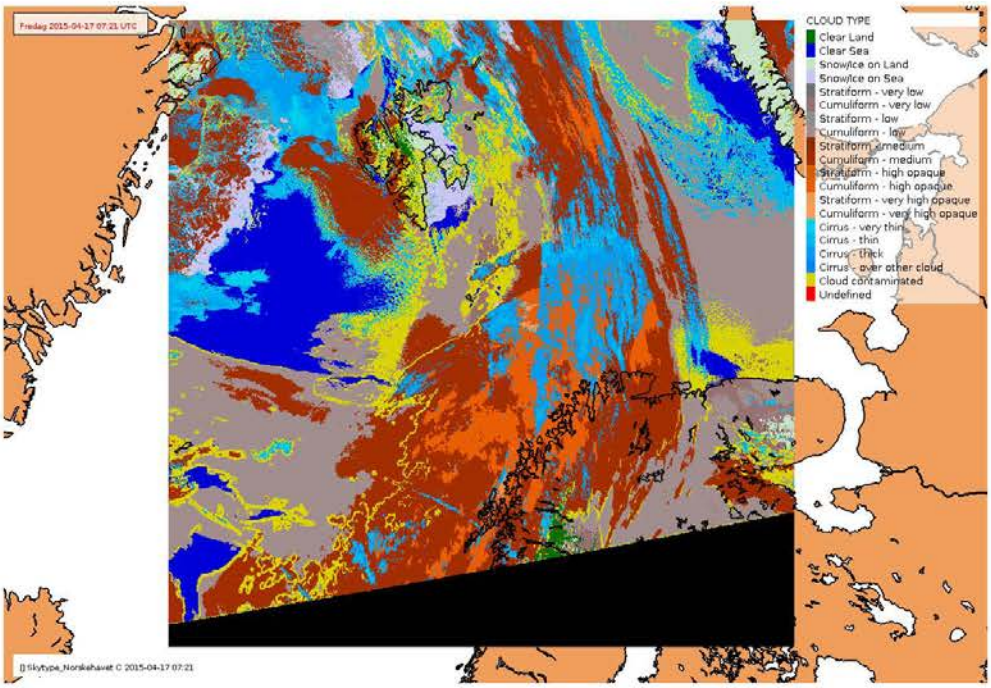

Figure 2. PPS cloud type classification of NOAA-19 image.

5

2.2 Synop-observations

Total cloud cover is observed at ~75 SYNOP locations in Norway by manual observers. Also automatic measurements exist, but are more commonly used in other countries, but are also tested in Norway [3]. Manual and automatic observations are in general similar, but might show different characteristics in certain aspects. A broader discussion of cloud cover from SYNOP observations is found in Mittermaier [4]. Here a few issues relevant for this study are repeated.

Manual observations of total cloud cover are described as 'the fraction of the celestial dome covered by all clouds visible' and depend on the visible horizon. This means that potentially the observations represent a large spatial area, much larger than satellite-based measurements (pixels of 1,5 x 1,5km) and forecasts from numerical weather prediction models (<20km)..

Total cloud cover is observed according to a given instruction [5]. Despite the instruction, manual observations make room for consistency problems between observers. Also a restricted hemispheric view at some locations influences the reported total cloud cover. Since the observations in Norway are done manually their uncertainty is larger during nighttime, than during daytime. The given instructions also indicate that there is an underreporting of 0/8 and 8/8 oktas (a small cloud on a almost clear sky or a small breakthrough of sun for total overcast are supposed to be reported as 1/8 and 7/8, respectively).

When compared to the cloud mask and different cloud cover forecasts we recalculate observed cloud cover from oktas to percentage [0 to 100%] cloud cover.

2.3 Comparison of synop-observation and cloud mask product

The cloud mask product is intended for maritime areas and this survey is restricted to ocean areas. We therefore limit us to use SYNOP-observations from Islands, but include also locations at the coast that are relatively exposed to open ocean (i.e. cloud mask product not contaminated by land) to increase the amount of observations. Table 3 shows the used SYNOP observations.

SYNOP-observations and cloud mask measurements are two estimates of the true cloud cover. However, they differ as they rarely are measured at exact similar times, are measured by different methods and represent different spatial scales. In Figure 3, we show the Mean Absolute Difference (MAD) and the Mean Difference (MD) between the SYNOP observations and the cloud mask product as function of month in 2014. The different lines in the Figure are the cloud mask product averaged over repeatedly larger squares around the SYNOP location.

The Mean Difference indicate that during summer (winter) there are on average more (less) clouds observed in the manual SYNOPs than in the cloud mask. We have not investigated why this systematic difference with season appears. The Mean Absolute Difference indicates that the correspondence between the two data sets is best in summer and worst in winter. It is also very clear that the correspondence between SYNOP and cloud mask product increase as the latter is averaged over larger areas. In our further use of the cloud mask product we use the cloud mask product averaged over 31 x 31 pixels (46,5km x 46,5km). We believe this is close to what the SYNOP-observations represent with respect to spatial scales.

WMO no	Name	Latitude	Longitude	Fylke	comments
1115	Myken	6.7628N	12.4860E	Nordland	Coast
1144	Helligvær	67.4048N	13.8958E	Nordland	Coast
1160	Skrova	68.1503N	14.6508E	Nordland	Coast
1010	Andøya	69.3073N	16.1312E	Nordland	Coast
1078	Gamvik II	71.0647N	28.2513E	Finnmark	Coast
1098	Vardø Radio	70.3705N	31.0958E	Finnmark	Coast
1003	Hornsund	77.0017N	70.9394E	Svalbard	Coast
1028	Bjørnøya	74.5167N	19.0050E	Svalbard	Ocean
1062	Hopen	76.5097N	25.0133E	Svalbard	Ocean
1001	Jan Mayen	70.9394N	8.6690W	Jan Mayen	Ocean

Table 3. SYNOP-sites used for verification

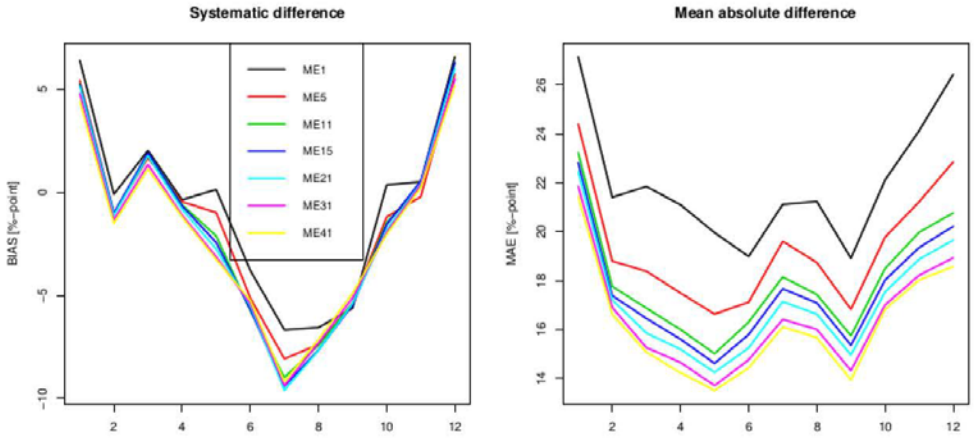

Figure 3. Systematic (left) and absolute difference (right) between all SYNOP observations in Table 3 and CM. CM is averaged over larger and larger squares centered around the SYNOP location. ME1 is the nearest CM pixel, while ME41 is averaged over 20 pixels in all directions.

3. Cloud Forecasts

3.1 Persistence of cloud mask product

For now-casting purposes it is often difficult to beat a persistence forecast. That is, you forecast what you observe at the moment to happen in the future. This can of course be done with different lead times and it is natural to think that the quality of such a forecast degrades rapidly with lead time. In this work we include persistence forecasts by simply using the CM product with 3hr lead time (pers3) and 6hr lead time (pers6). The two different lead times is used to illustrate at which rate a persistence forecast is degraded.

3.2 Advected cloud mask product

3.2.1 Input data

To be able to do cloud advection we need wind data for the same area and period. We get this data from a Numerical Weather Prediction (NWP) model, namely HIRLAM12 [2]. These files are available

in the so-called 'felt' format and so are first converted to NetCDF files, similarly to what we do with the cloud data. They are also re-gridded to our selected product area during this conversion process.

We have four of these model files for each day with analysis times 00, 06, 12 and 18. These files contain the wind speed for each cell in the target area projected onto the x- and y-axis. These x_wind/y_wind variables also have seven different pressure (vertical) levels, or heights, and four times. These pressure levels are 300, 400, 500, 700, 850, 925 and 1000 hPa and the times are from 3 to 12 hours after the model file's analysis time in four 3hr increments. So for instance, the h12pl12_20141211.nc4 model file would contain the predicted wind fields for 15:00, 18:00, 21:00 and 00:00.

As will be seen in the algorithm section next we will be using the 925, 700 & 500hPa wind layers for our purposes. 500hPa is roughly halfway to the tropopause and so gives an altitude of around 5.5km, 700hPa is closer to 3km and lastly 925hPa corresponds to around 0.75km.

3.2.2 Advection Algorithm

When advecting the clouds we use the cloud type product from PPS rather than the cloud mask product. This gives the advantage of being able to separate the clouds into three different height layers from their type classification and then advecting the layers with different winds.

Unless otherwise stated the programming language used during this entire section (as well as for the previously mentioned HDF → NetCDF conversion of the input files) is Python. Figure 4 shows an overview of the steps taken starting from our initial input files and up to the cloud forecast is generated. The last half of that chart is actually repeated several times as will be explained in the section on the hourly steps in the algorithm.

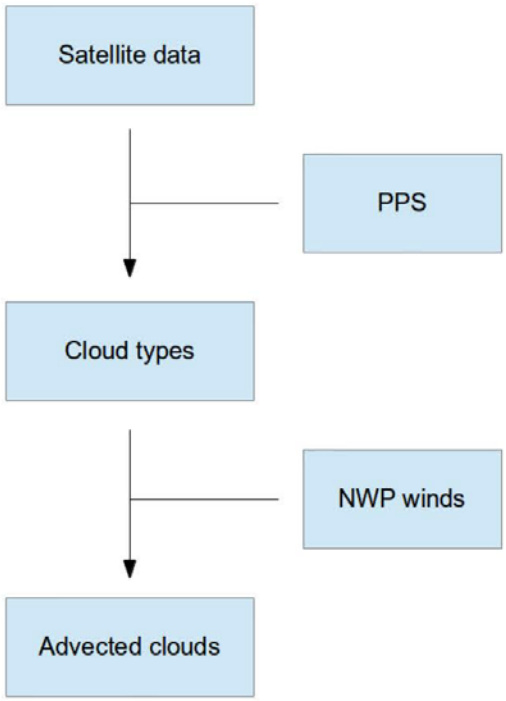

Figure 4. Simplified chart showing the advection process.

3.2.3 Selecting winds

The first step is splitting the cloud layer into three different heights based on the cloud category: low, medium and high. In addition to these layers we have the cloud-free area and the previously mentioned undefined area where the cloud type variable is undefined.

We select the 925hPa, 700hPa and 500hPa winds to advect our low, medium and high cloud layers respectively. To simulate the uncertainty of clouds moving into our area from outside, we advect the boundary edge with the greatest wind speed for those cells to move an unknown area in from the edges. This unknown field may gradually obscure parts of the area depending on the wind direction. We also advect the cloud-free area with the 'ground' wind for technical reasons to simulate an area opening up when clouds move away from a cell.

This type of cloud advection is of course very basic as it does not take into account any cloud formation or dissipation. Also, for each hourly step when we generate the new cloud type we just select the nearest layer, so if a medium and high layer happen to converge then only the nearest layer is kept in that cell.

Next we need to select the model wind for the time period we are in. To do this we find the most recent model file that is at least 3hrs older than our satellite time (since the model files only contain

wind predictions starting 3hrs ahead). From this file we select the wind from the last 3hr period to advect our cloud field.

So if we were advecting a cloud field from 12:40 to 13:00 we would be using the 12:00 wind prediction from the 06:00 analysis file. We could have interpolated the 12:00 and 15:00 winds, but in the interest of supporting a potential operational situation where later wind fields are unavailable we only used the last wind field before the satellite time. This is of course another source of uncertainly in the algorithm, that the winds we use will also be outdated in addition to the model uncertainty.

3.2.4 Hourly steps

The forecast variable we generate in the NetCDF file is for 6 times. The first forecast time is the first full hour after the satellite time, so may be as little as a few minutes after the satellite time up to a full hour. The next five forecasts are then the full hours after the first forecast. This means that the forecast can vary from 5 to 6 hours in the files. The 'time' variable in the files gives the exact times of these forecast steps just as the 'forecast_reference_time' variable gives the satellite time.

For each forecast we first select the winds from the model file as described above. We then use those winds to move the clouds from their starting position given by the grid cells to new positions. Different winds are used in different cells depending on the cloud layer in that cell. This starting cloud status is defined by the cloud cover variable if it's the first forecast, otherwise we use the previous forecast as the starting cloud status. We then use a gaussian k-d tree resampling to get the values in our target grid for the forecast from our advected field.

The next step is handling the movement of the unknown mask from the edges separately with a C-library using Bresenham's line algorithm. This masks the path as well as the ending point. As may be seen from the forecasts this can manifest as 'contour' lines if clouds from a cloud layer inside our area have the opposite direction and overlap the unknown mask.

Next we need the resulting cloud types from the advection. We already have the cloud cover forecast from our first step as a percentage, but we need the types as well so we can split the clouds into layers. This needs to be done so we can select the correct winds for the grid cells for the next forecast step, just as we did for the previous. To accomplish this we use a nearest neighbor resampling from the new positions to our target grid positions. As mentioned earlier this may lead to a loss of cloud data in areas where different cloud types converge, and a growth where they diverge.

The final step consists of filling in grid cells of the cloud forecast where no cloud data is present due to divergences. Much like for the cloud type we use a k-d tree approach to do the filling based on the neighboring grid cells.

3.2.5 Write results to file

With the hourly steps finished and the full forecast generated we write the results to our NetCDF file. In addition to the cloud_forecast variable this includes the model_wind_reference_time that has the absolute time of the model file with the winds used for the cloud advection.

3.2.6 A first comparison

In this section we will briefly look at a few examples where we compare the cloud cover as given by

10

the PPS software to a forecast of the approximate same time from a file 3hrs earlier. We've randomly selected the date 2014-06-06 and we will look at MetOp-A, NOAA-18 and NOAA-19 examples. This is meant merely as a quick visual representation, as the validation part of this report will deal with the quality assessment.

The first two figures are for MetOp-A. The masked area can be quite large in the figures as it's the combination of the mask in the cloud forecast from the earlier file (where the edge area has been allowed to move inwards) and the cloud cover mask in the later file.

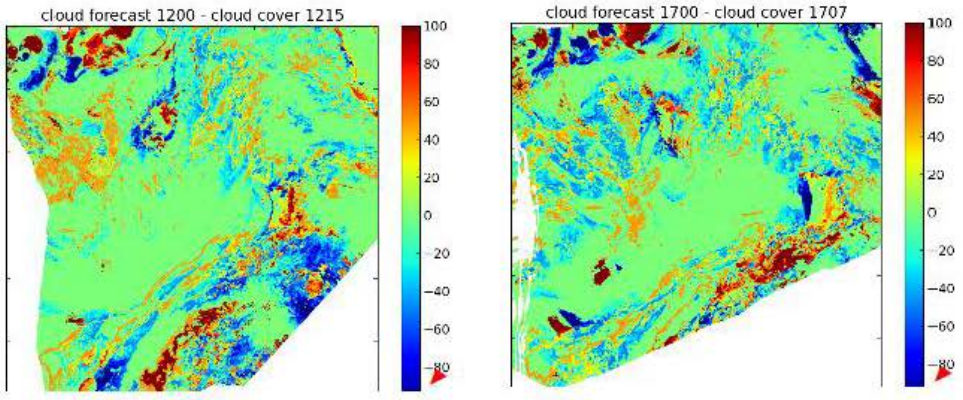

Figure 5 MetOp-A

A value of 100 in these figures means that our forecast says there should be 100% cloud while the cloud cover says there are no clouds there. A value of -100 naturally indicates the opposite. This mostly happens along the cloud edges where the smoothing of the nearest neighbor resampling comes into effect.

Next we have two figures for NOAA-18 (Figure 6) and one from NOAA-19 (Figure 7).

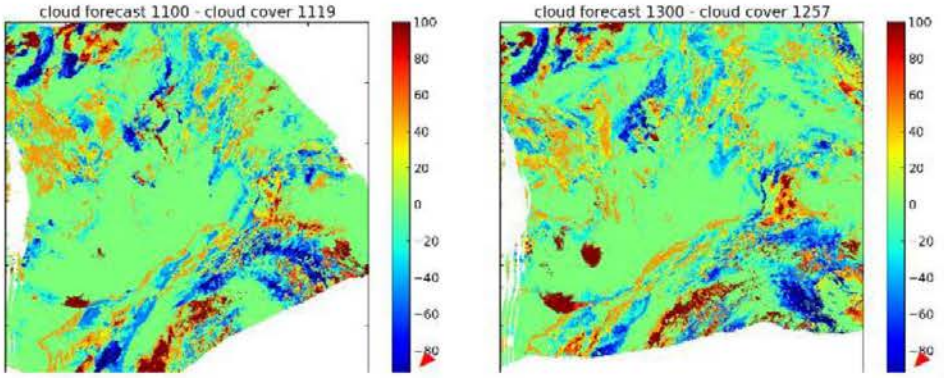

Figure 6. NOAA-18

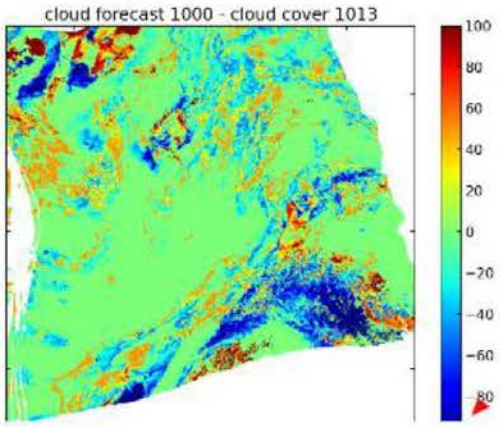

Figure 7: NOAA-19

These figures all generally show the same. Large areas with cloud mostly remain cloudy in a 3hr forecast while the edges and small cloud-free areas have a greater tendency to differ between the forecast and the later cloud cover. Areas within clouds that may open up are another type of process that won't be simulated with the current algorithm as well as clouds moving in from outside the edges of our product area.

In the following we use the short-name AdvCM3 for forecasts based on advection of the cloud mask product with a lead time of 3hr.

3.3 ECMWF

This is the Numerical Weather Prediction Model from the European Center for Medium Weather Forecast (www.ecmwf.int). The model has a global coverage and a grid resolution of approximately 16km for the areas of interest here. At MET-Norway the model forecasts are available approximately 6-7hr after initial time and the model are updated 4 times daily (00, 06, 12 and 18UTC).

The model is under continuously development and a new model version is planned for operational use in May 2015. In addition, ECMWF plan another model upgrade later in 2015 or 2016 that increases the grid resolution of the model.

In addition to the ECMWF model, MET-Norway runs several other models, i.e. the AROME-MetCoOp which is the basis of the official forecasts from MET-Norway (i.e. at Yr.no). This model is at approximately the same level as ECMWF with respect to quality of cloud forecasts, but is employed only over a limited region close to Norway and do not cover the entire area of interest in this project.

4. Norwegian Cloud Climatology

Observed Cloud Cover climatology from Norwegian SYNOP stations are shown in Figure 8. In yearly average the Total Cloud Cover (TCC) is higher over ocean than land areas. There is also less temporal variability in TCC over the ocean. In the following we only describe the TCC climatology over ocean. The three most northern situated stations (Jan Mayen, Bjørnøya and Hopen) has yearly average cloud clover between 6 and 7 oktas and more clouds in summer than in winter. However, for the stations situated closer to the Norwegian west coast (typically connected to oil installations) there are slightly lower yearly averages. In addition, for these areas we see the opposite yearly cycle and more clouds are observed during winter. At coastal stations the average TCC is slightly smaller or equal to what is observed further out in the ocean.

In appendix B a detailed cloud cover distribution for all seasons is plotted for each station. There is a clear tendency that the major observed cloud categories are 8 and 7 oktas, which are seen for all stations.

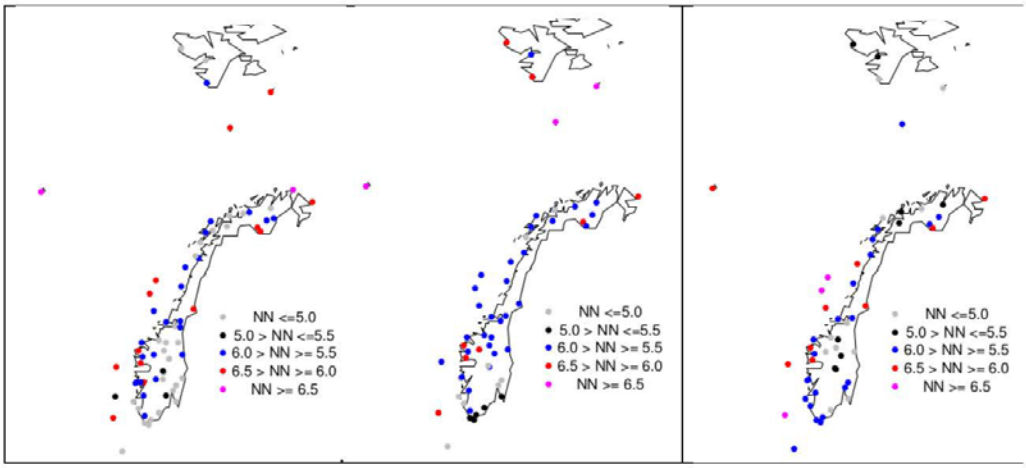

5. Verification against cloud mask product

The now-casting products pers3 (3hr persistence), pers6 (6hr persistence) and AdvCM3 (advection of cloud mask product with lead time of 3hr) have their entire basis in CM (cloud mask product). They therefore inherit some of the same characteristics as CM and have the same spatial resolution. It is therefore natural to evaluate these forecasts with CM. However, due to the spatial issues and the close relationship between pers3, advCm3 and CM we omit the ECMWF in this part of the evaluation.

In the first row of Figure 9, the 2014 average for pers3 and AdvCM3 is plotted. As with the observed SYNOP climatology these plots confirm that this is in general a cloudy area, but that there also are quite some regional differences (i.e. less clouds to north east). We also see that the areas associated with high averages of TCC are also associated with less variability. Further, AdvCM3 is smoother than pers3, which has kept the small scale details from the CM.

Mean Absolute Error (MAE) for pers3 and AdvCM3 (compared to CM) are shown in the second row of Figure 9. MAE varies largely with in the evaluation domain (from approximately 10 to 30%-points). Smaller errors are found in areas with high average cloud cover and less observed variability. On average AdvCM3 have larger errors than pers3 (highlighted in Figure 10). This is especially true for the areas to south west ant north east of the domain. For the ocean areas between Norway and Spitsbergen and west of Spitsbergen they are almost equal or slightly in favor of AdvCM3.

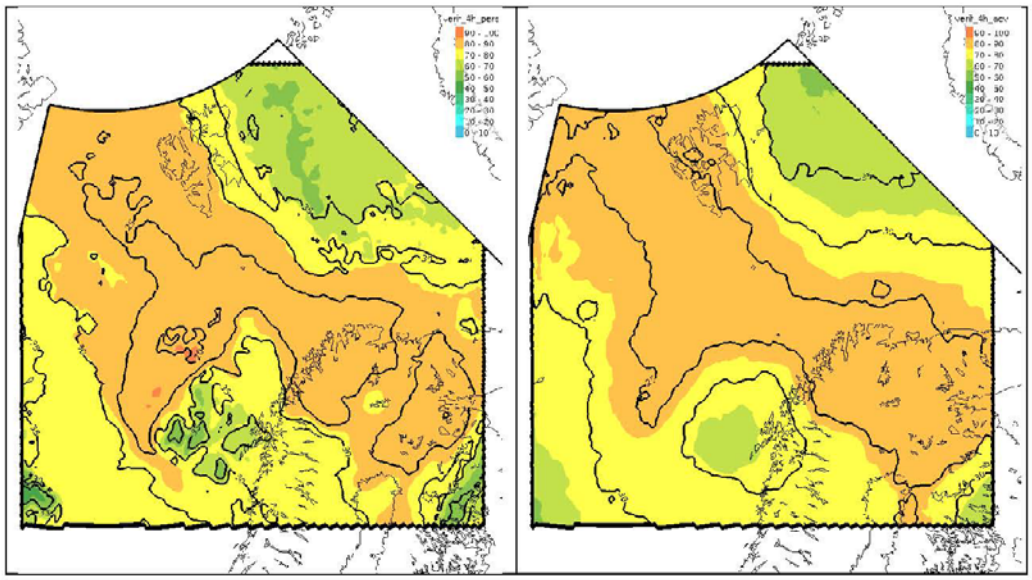

15

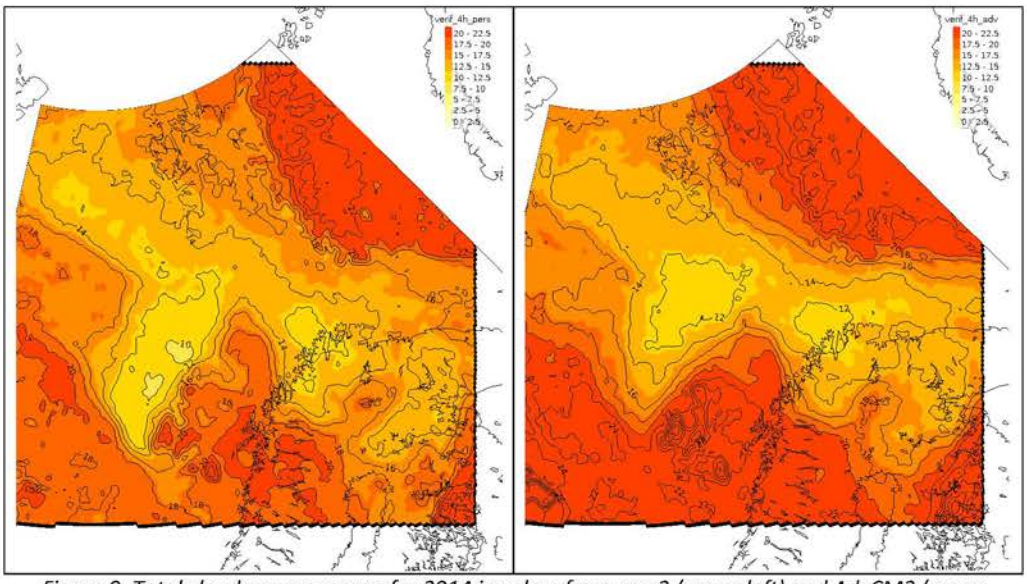

Figure 9. Total cloud cover average for 2014 in colors from pers3 (upper left) and AdvCM3 (upper right). Black lines indicate standard deviation of the forecast. The lower row show mean absolute error (MAE) against the cloud mask product for pers3 (left) and AdvCM3 (right).

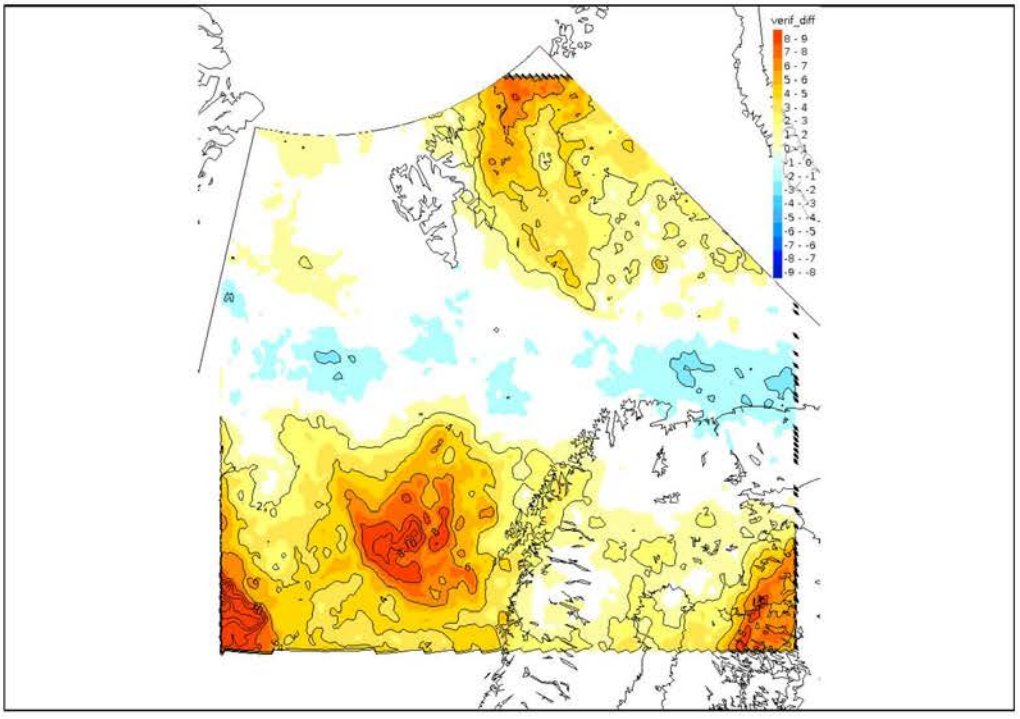

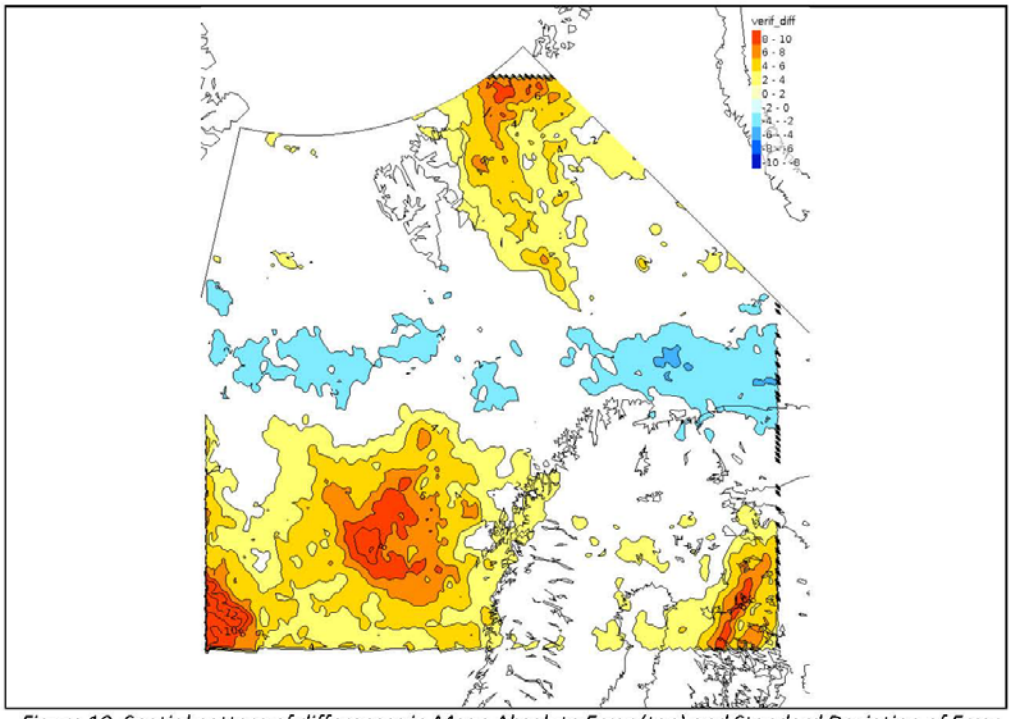

Figure 10. Spatial pattern of differences in Mean Absolute Error (top) and Standard Deviation of Error (bottom) between pers3 and AdvCM3. Warm colors (yellow/red) indicate lower errors in pers3 than in AdvCM3.

6. Verification against Synop-observations

6.1 Ocean stations.

The SYNOP observations of TCC are independent of the forecast products pers3, pers6, advCM3 and ECMWF. We can therefore compare the quality of the forecast products. However, to take into account the differences in spatial scales we average pers3, pers6 and advCM3 as described in chapter 2.

Figure 11 shows the systematic error (bias), Mean Absolute Error (MAE), Standard Deviation of the Error (SDE) and the correlation (COR) for an average for 2014 over the three ocean stations Jan Mayen, Bjørnøya and Hopen. ECMWF has slightly more clouds than the SYNOPs, while the CM-based products have slightly less. Pers3 performs best for all measures, while pers6 performs worst. This illustrates a fast degradation of a persistence forecast.

Figure 12 summarize how well the different forecast products are able to forecast events with less than 50% cloud cover. In this particular example 50% cloud cover is chosen, but qualitatively we se the same effect for other thresholds. On average pers3 and advCM3 is of similar quality, but shows slightly different characteristics. Pers3 forecast correctly a larger part of the observed events (higher hit rate), but do also have a larger false alarm ratio. ECMWF and pers6 are clearly not as good as the two other forecast products. ECMWF is slightly better than pers6.

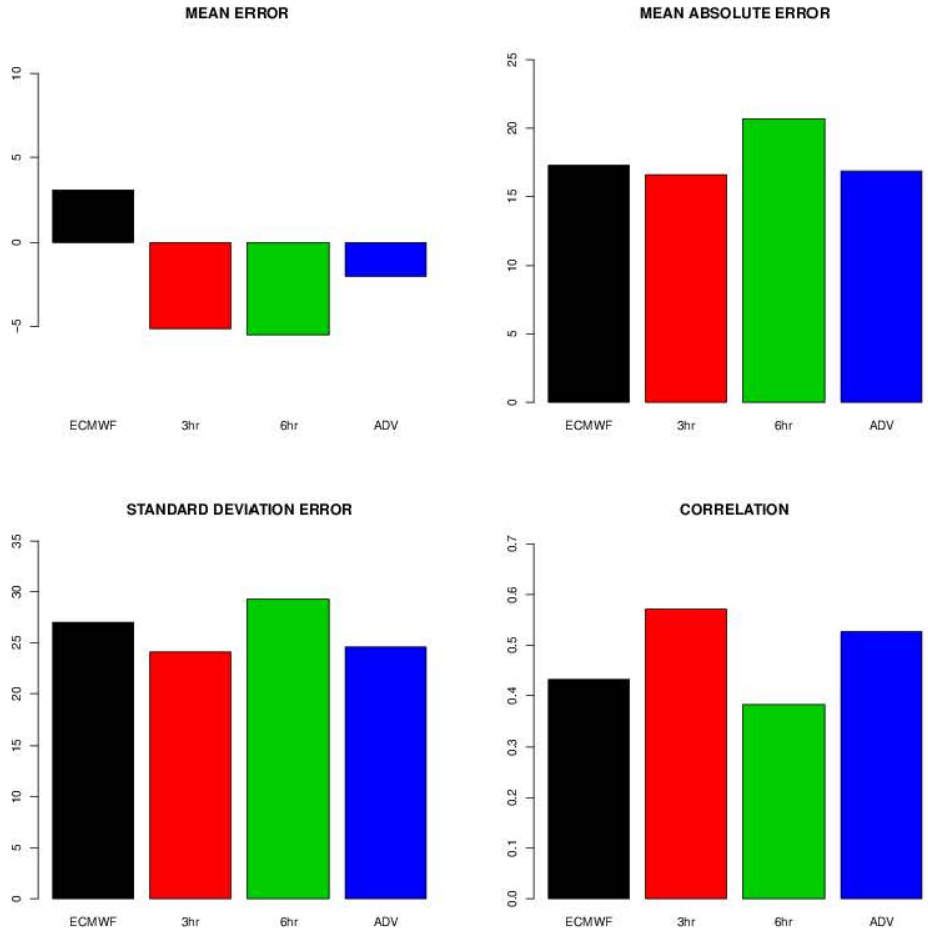

Figure 11. Verifications scores (Mean Error, Mean Absolute Error, Standard Deviation of Error and Correlation, see appendix A) for ocean stations (Jan Mayen, Hopen and Bjørnøya) for 2014.

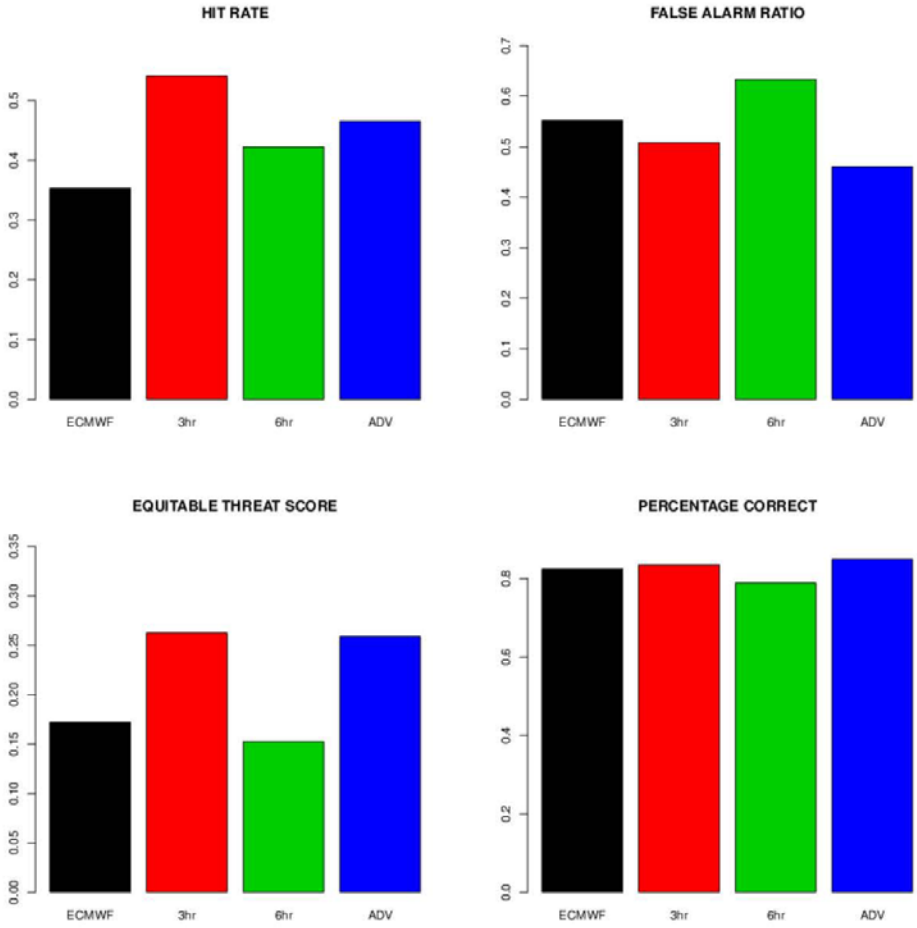

Figure 12. Threshold verification (Hit rate, False Alarm Ratio, Equitable Threat Score, Percentages Correct, see appendix A) for ocean station in 2014.

6.2 Coast stations.

Figure 13 shows the systematic error (bias), Mean Absolute Error (MAE), Standard Deviation of the Error (SDE) and the correlation (COR) for an average for 2014 over the coast stations listed in table 3. ECMWF, pers3 and pers6 has slightly less clouds than the SYNOPs, while advCM3 has almost no systematic error. Pers3 performs clearly best for all three measures, while pers6 and ECMWF performs worst.

Figure 14 summarize how well situations with less then 50% cloud cover are forecasted. Other thresholds give qualitatively similar results. On average pers3 outperform the other forecast products with higher hit rate, equitable threat score and percentages correct and lower false alarm

ratio. ECMWF, pers6 and advCM3 is very similar in total quality but differs in their characteristics. ECMWF show larger hit rate and false alarm ratio than the pers6 and advCM3.

In appendix C similar plots for each season is plotted (averaged over all ocean and coast stations). The results described above are fairly consistent for all seasons. However the largest errors are found in winter and spring.

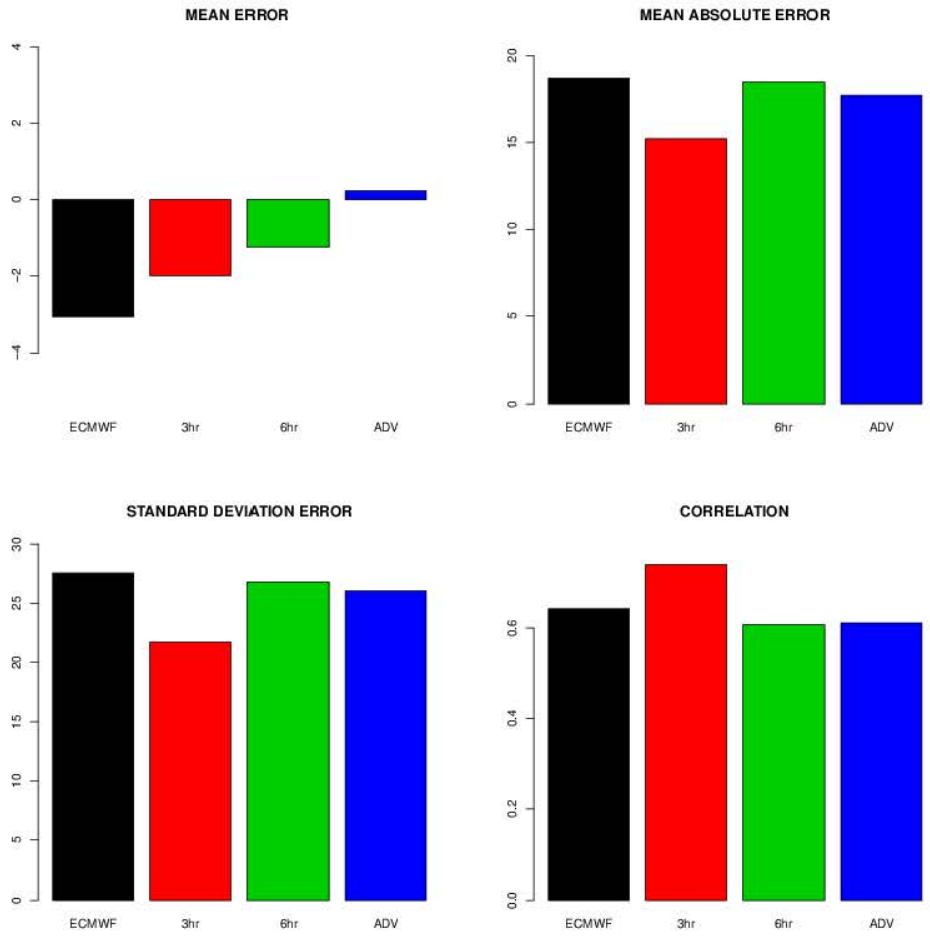

Figure 13. Verifications scores (Mean Error, Mean Absolute Error, Standard Deviation of Error and Correlation, see appendix A) for coast stations for 2014.

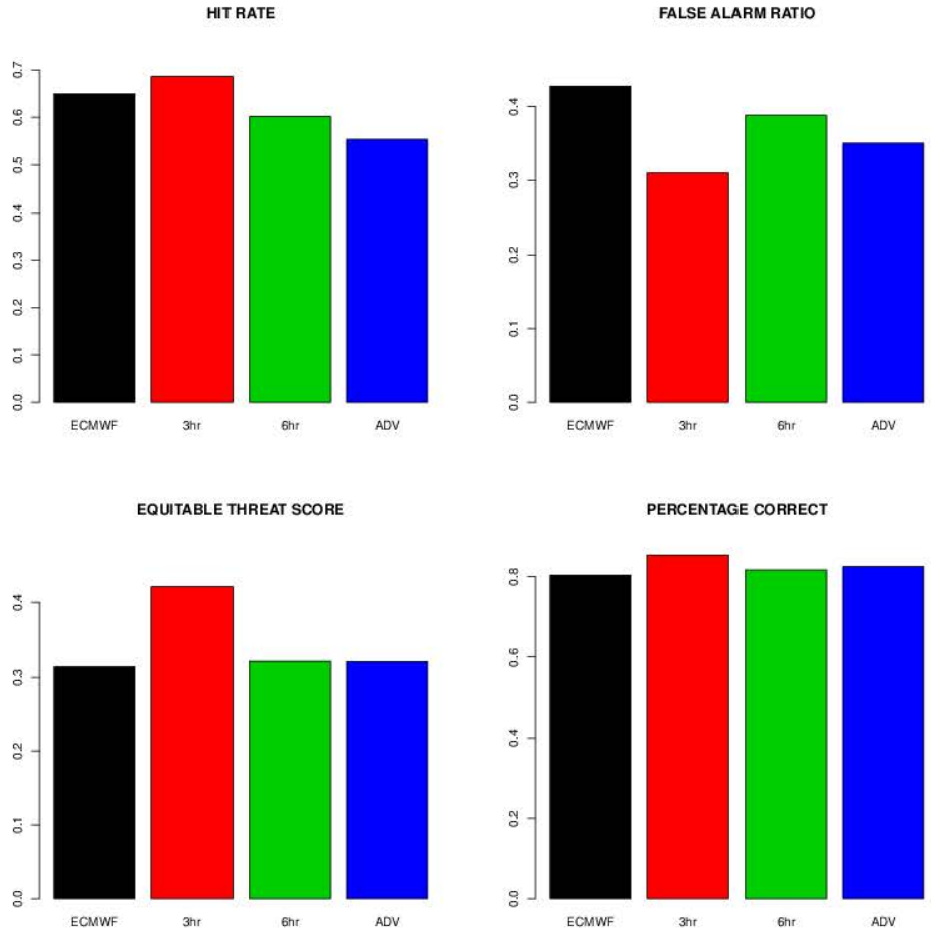

Figure 14.. Threshold verification (Hit rate, False Alarm Ratio, Equitable Threat Score, Percentages Correct, see appendix A) for coast station in 2014.

21

7. Summary

The objective of this study has been to investigate the quality of now-casting (2 to 4hr ahead) of cloud cover in maritime areas. Two independent observation sources of cloud cover have been used, namely manual SYNOP-observations and a satellite-based cloud mask product.

In general weather forecasting at MET-Norway employ NWP models. In this study only the ECMWF-model has been used as the main model at MET-Norway, AROME-MetCoOp), only cover a minor part of the area of interest. In addition, persistence forecasts (two different lead times, +3hr and +6hr) based on the cloud mask product has been used as a baseline forecast. Finally, also an advection of the cloud mask product using wind information from a NWP model has been developed and compared to the rest of the available cloud cover forecasts.

Average cloud cover for 2014 has been calculated from the cloud mask product, while observation series (up to 30year) has been used for similar calculations for the SYNOP-observations. The results reveal a high average cloud cover for the ocean areas studied (6-7 oktas). At the Norwegian coast, the average cloud cover is slightly lower with a higher temporal variability.

The cloud mask based forecast products has been evaluated against the cloud mask itself. This comparison reveals that the quality varies somewhat between regions. The forecast quality increases in regions with less observed variability. The comparison shows that on average 3hr persistence forecast performs better than a 3 hour advected cloud mask product.

All described cloud mask based forecast products have further been verified against SYNOP-observations, which is independent for all of the forecasts. The results from this comparison confirm the quality difference between 3hr persistence forecast and the 3 hour advected cloud mask. In addition, the comparison shows that a 3hr cloud mask based persistence forecast also performs better than forecasts from the ECMWF model. However, already at lead times of 6hrs the cloud mask based persistence forecast performs worse compared to the forecast from the NWP model and the advected cloud mask. These findings with respect to the quality of the cloud mask based persistence forecast are in agreement with previous experiences from now-casting.

Results from this study show that now-casting based on persistence from satellite -based cloud masks show higher skill than other presently tested methods. However, as NWP model systems develop, and i.e. dedicated NWP now-casting system is constructed, it is reasonable to believe that this conclusion will be challenged.

References

[1] http://nwcsaf.smhi.se/Software.php

[2] http://www.hirlam.org/index.php/hirlam-programme-53

[3] https://nmm2014.files.wordpress.com/2014/05/borg_ceilometercomparison.pdf

[4] Mittermaier M. 2012. A critical assessment of surface cloud observations and their use for verifying cloud forecasts.Q. J. R. Meteorol. Soc.138 : 1794 – 1807. DOI:10.1002/qj.1918

[5] http://orap.met.no/Orap/Kodeforklaring/Obsveil/koder/Nddff_3.html

[6] http://www.cawcr.gov.au/projects/verification/

Appendix A: Description of verification methods.

There exists no single verification measure that covers all aspects of weather forecasts. However, it exist many different verification measures that highlight different characteristics of a weather forecast. In this study a set of 8 measures are used. For a mathematical formulation and discussion of all scores see i.e. [5]. Here only a brief description is given.

Systematic error (bias)

Measure the average error, the difference between the mean of the forecast and the mean of the observations. It is possible to achieve perfect scores if compensating errors are present.

Standard Deviation (SDE)

Measure the variation of the error around the systematic error. Interpret as unsystematic errors and perfect score is 0. Large deviations are emphasized (squaring of the error).

Mean Absolute Error (MAE)

Measure the mean average error and perfect score is 0.

Correlation

Measure how well did the forecast values correspond to the observed values.

Hit Rate (HR)

Measure the proportion of observed events that are correct forecasted. Score from 0 to 1, perfect score is 1. Ignores the false alarms and one can easily obtain high scores at all times by always forecasting events. HR can only be used together with other scores (i.e. FAR).

False Alarm Ratio (FAR)

Measure the proportion of forecasted events that did not occur (percentage of miss). Score from 0 to 1, perfect score is 0. Ignores the correct forecasts and will give perfect score if an event is never forecasted. FAR can only be used together with other scores (i.e. HR).

Equitable Threat Score (ETS)

Measure the number of correct forecasts for an event divided by the total number of observed and forecasted events and adjusted for correct forecasts due to chance. Score from -1/3 to 1, perfect score is 1. No quality gives 0. ETS penalties "non forecasted events" and "forecasted events, but not observed" similar.

Appendix B: Detailed cloud climatology for Synop-observations

Detailed cloud climatology for Bjørnøya (99710), Hopen (99720), Jan Mayen (99950), Myken (80610), Helligvær II (82410), Andøya (87110), Gamvik II (96560), Vardø Radio (98550) and Hornsund (99754).

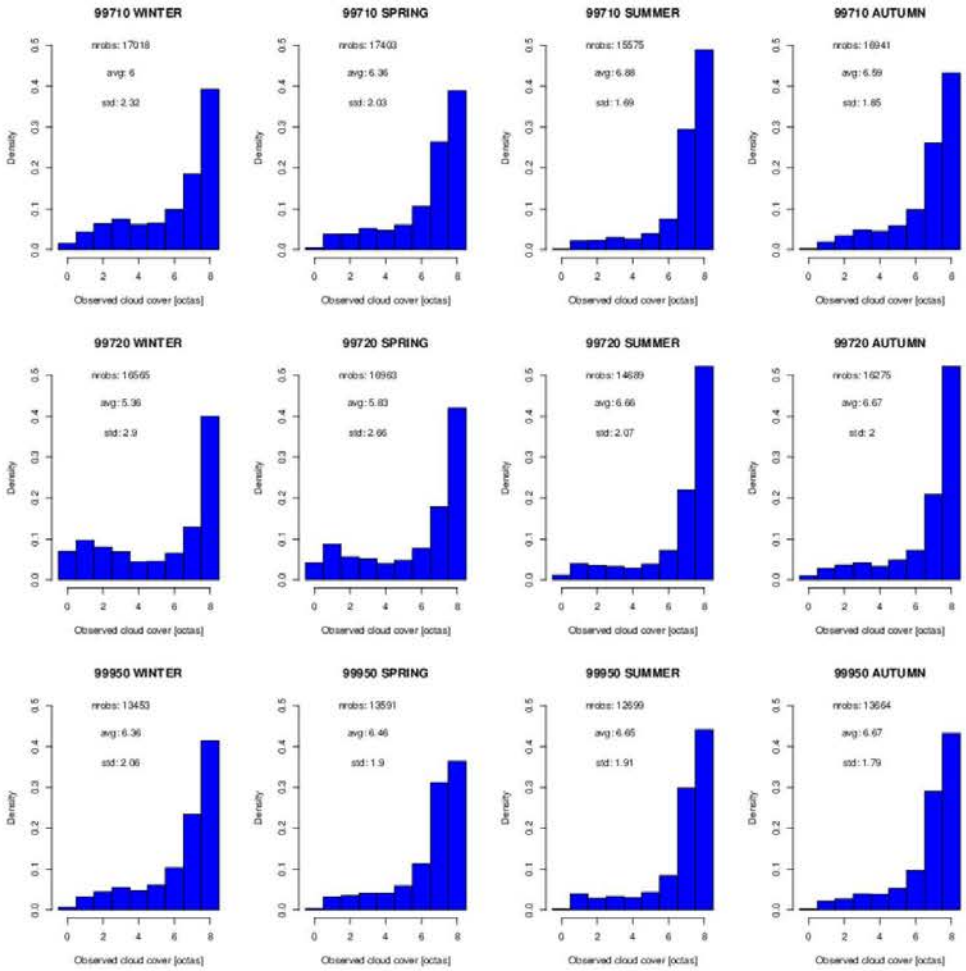

25

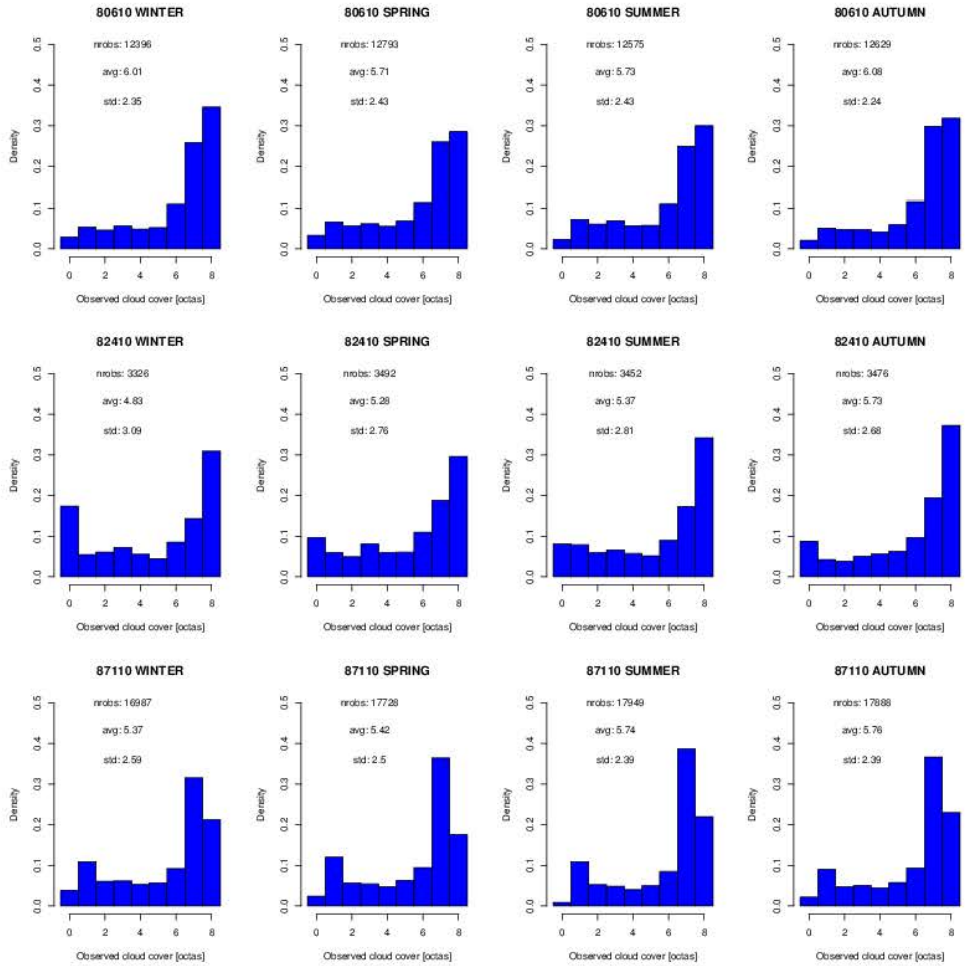
80610 WINTER
nrobs: 12396
avg: 6.01
std: 2.35
80610 SPRING
nrobs: 12793
avg: 5.71
std: 2.43
80610 SUMMER
nrobs: 12575
avg: 5.73
std: 2.43
80610 AUTUMN
nrobs: 12629
avg: 6.08
std: 2.24
82410 WINTER
nrobs: 3326
avg: 4.83
std: 3.09
82410 SPRING
nrobs: 3492
avg: 5.28
std: 2.76
82410 SUMMER
nrobs: 3452
avg: 5.37
std: 2.81
82410 AUTUMN
nrobs: 3476
avg: 5.73
std: 2.68
87110 WINTER
nrobs: 16987
avg: 5.37
std: 2.59
87110 SPRING
nrobs: 17728
avg: 5.42
std: 2.5
87110 SUMMER
nrobs: 17949
avg: 5.74
std: 2.39
87110 AUTUMN
nrobs: 17888
avg: 5.76
std: 2.39
Density
Observed cloud cover [octas]

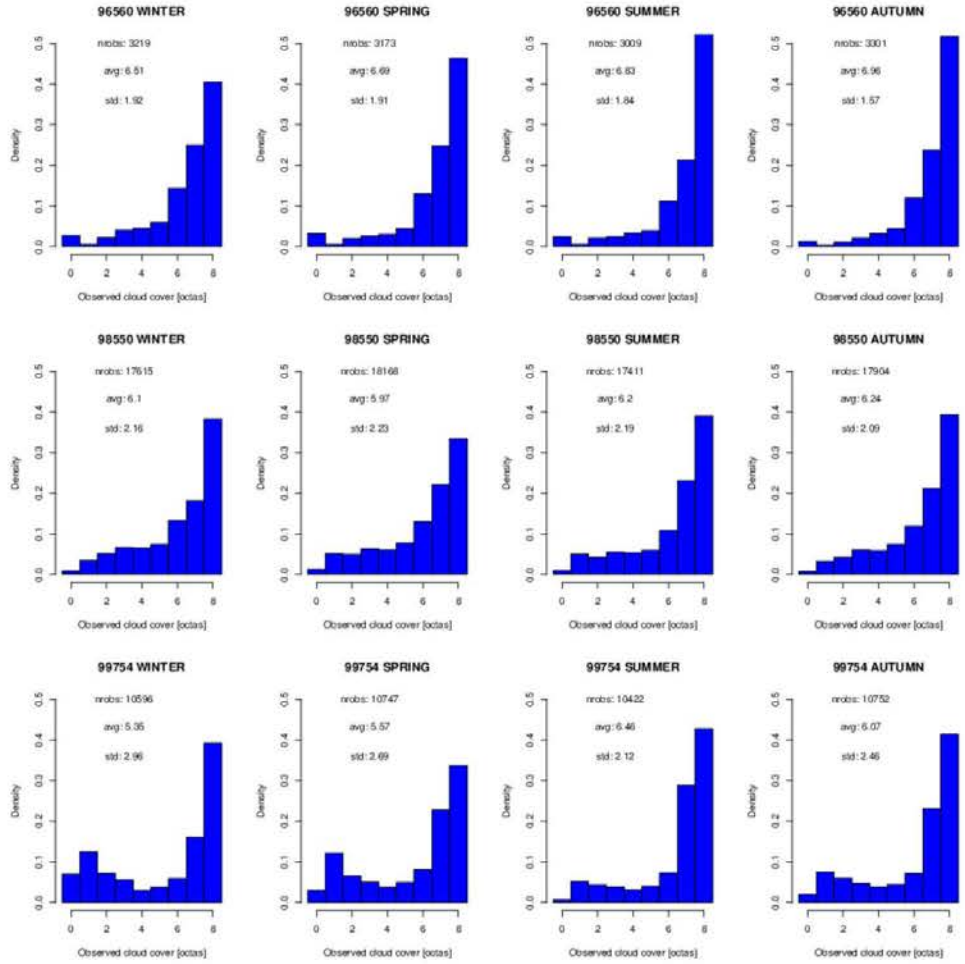
96560 WINTER
nrobs: 3219
avg: 6.51
std: 1.92
96560 SPRING
nrobs: 3173
avg: 6.69
std: 1.91
96560 SUMMER
nrobs: 3009
avg: 6.83
std: 1.84
96560 AUTUMN
nrobs: 3301
avg: 6.96
std: 1.57
98550 WINTER
nrobs: 17615
avg: 6.1
std: 2.16
98550 SPRING
nrobs: 18168
avg: 5.97
std: 2.23
98550 SUMMER
nrobs: 17411
avg: 6.2
std: 2.19
98550 AUTUMN
nrobs: 17904
avg: 6.24
std: 2.09
99754 WINTER
nrobs: 10596
avg: 5.35
std: 2.96
99754 SPRING
nrobs: 10747
avg: 5.57
std: 2.69
99754 SUMMER
nrobs: 10422
avg: 6.46
std: 2.12
99754 AUTUMN
nrobs: 10752
avg: 6.07
std: 2.46
Density
Observed cloud cover [octas]

27

Appendix C: Seasonal verification plots

SUMMER:

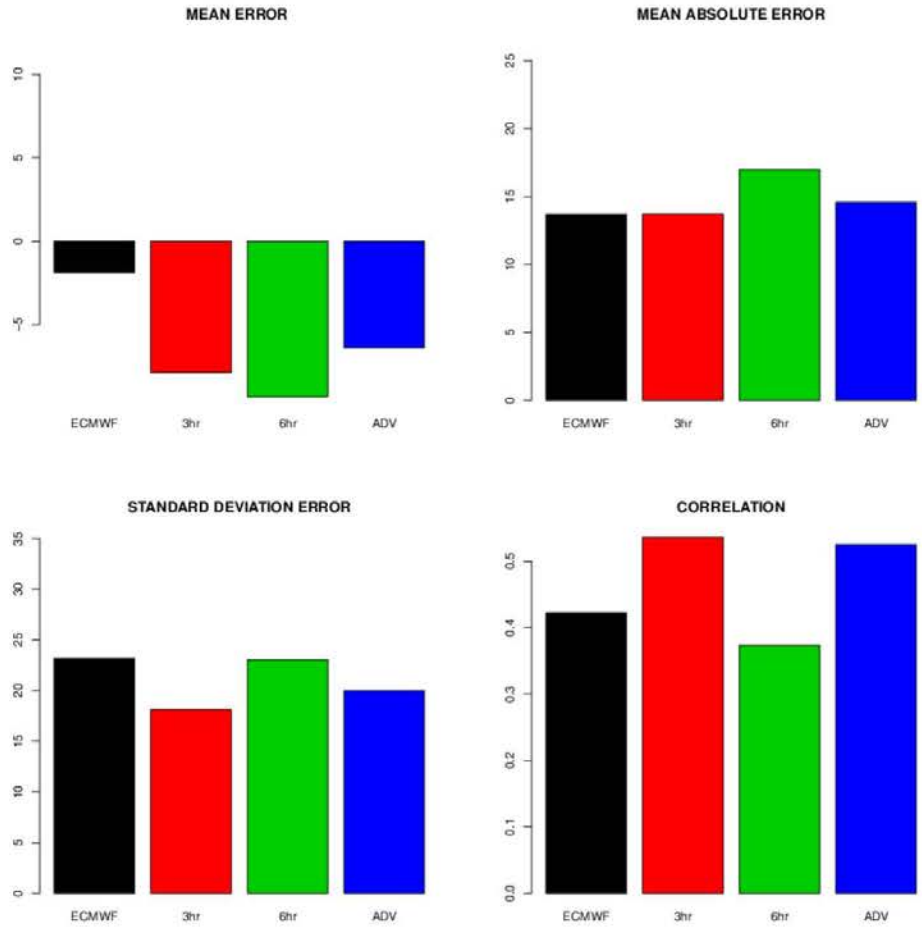

28

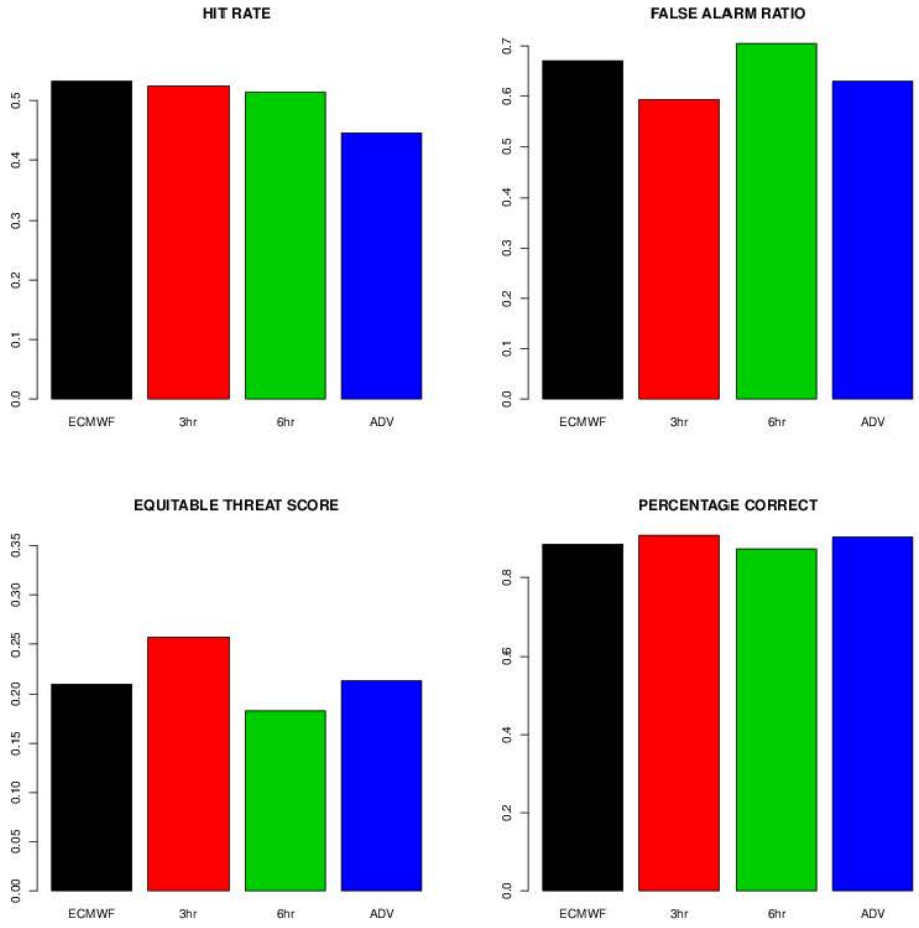
HIT RATE
0.0
0.1
0.2
0.3
0.4
0.5
ECMWF
3hr
6hr
ADV
FALSE ALARM RATIO
0.0
0.1
0.2
0.3
0.4
0.5
0.6
0.7
ECMWF
3hr
6hr
ADV
EQUITABLE THREAT SCORE
0.00
0.05
0.10
0.15
0.20
0.25
0.30
0.35
ECMWF
3hr
6hr
ADV
PERCENTAGE CORRECT
0.0
0.2
0.4
0.6
0.8
ECMWF
3hr
6hr
ADV

29

AUTUMN:

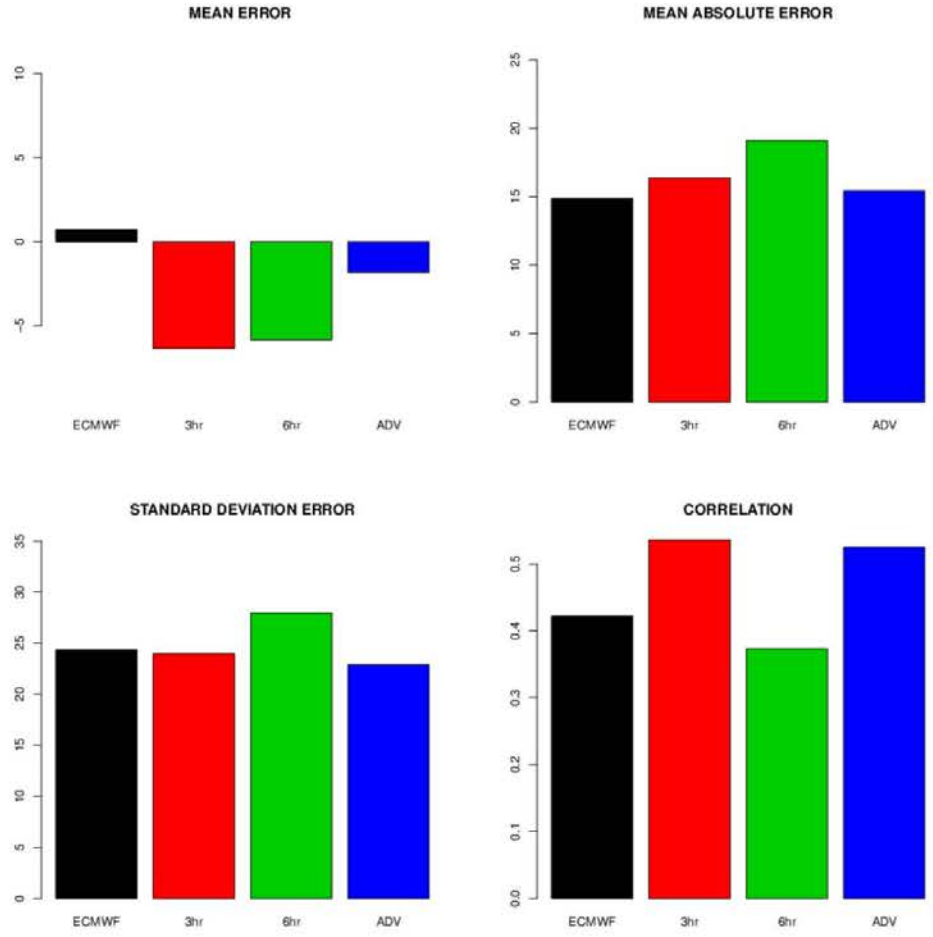
MEAN ERROR
10
5
0
-5
ECMWF
3hr
6hr
ADV
MEAN ABSOLUTE ERROR
25
20
15
10
5
0
ECMWF
3hr
6hr
ADV
STANDARD DEVIATION ERROR
35
30
25
20
15
10
5
0
ECMWF
3hr
6hr
ADV
CORRELATION
0.5
0.4
0.3
0.2
0.1
0.0
ECMWF
3hr
6hr
ADV

30

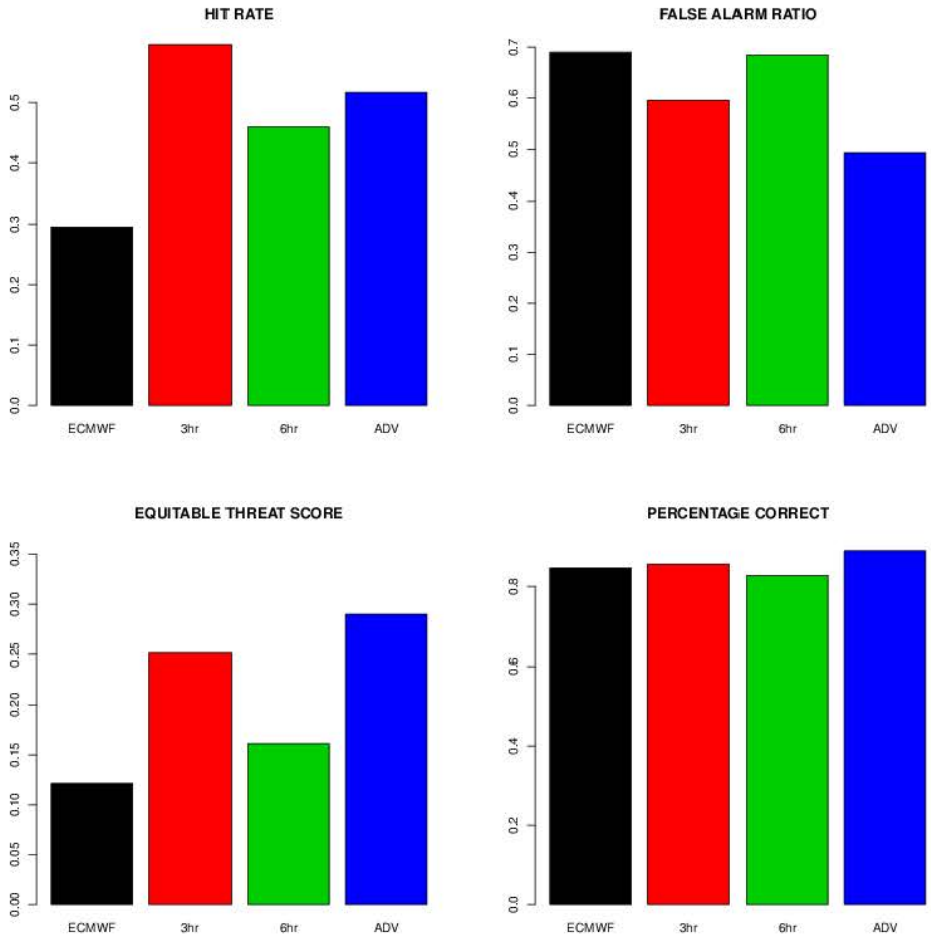
HIT RATE
0.0
0.1
0.2
0.3
0.4
0.5
ECMWF
3hr
6hr
ADV
FALSE ALARM RATIO
0.0
0.1
0.2
0.3
0.4
0.5
0.6
0.7
ECMWF
3hr
6hr
ADV
EQUITABLE THREAT SCORE
0.00
0.05
0.10
0.15
0.20
0.25
0.30
0.35
ECMWF
3hr
6hr
ADV
PERCENTAGE CORRECT
0.0
0.2
0.4
0.6
0.8
ECMWF
3hr
6hr
ADV

31

WINTER:

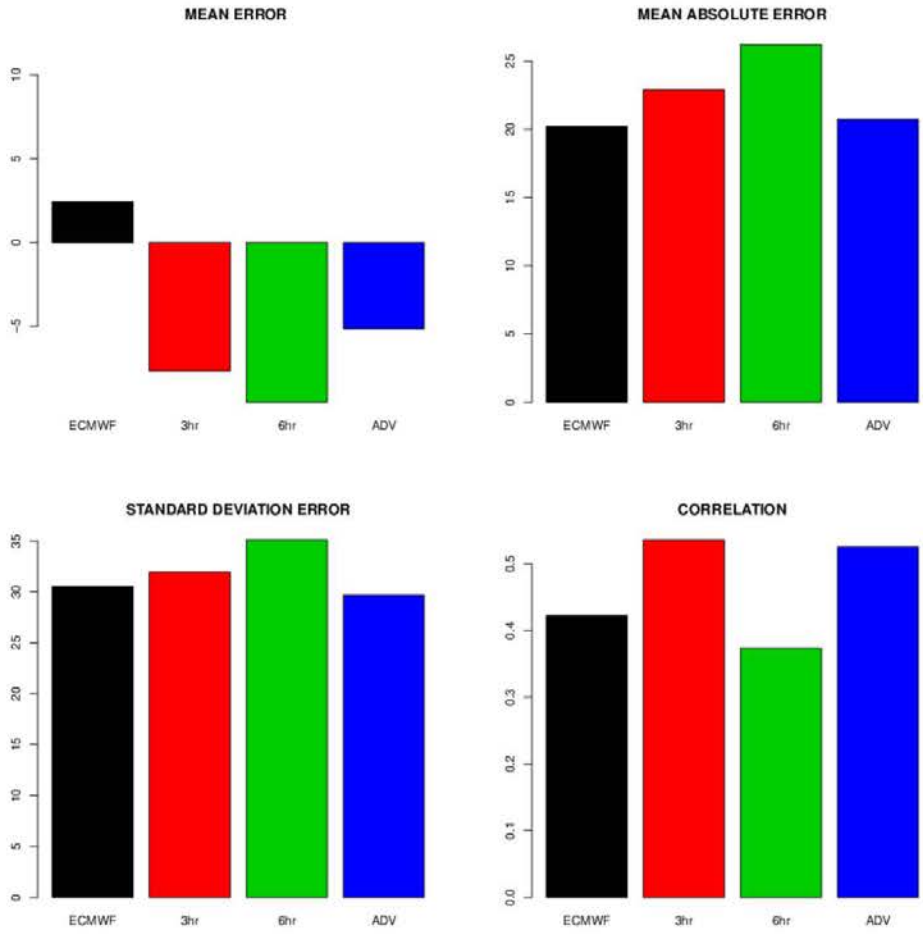
MEAN ERROR
10
5
0
−5
ECMWF
3hr
6hr
ADV
MEAN ABSOLUTE ERROR
25
20
15
10
5
0
ECMWF
3hr
6hr
ADV
STANDARD DEVIATION ERROR
35
30
25
20
15
10
5
0
ECMWF
3hr
6hr
ADV
CORRELATION
0.5
0.4
0.3
0.2
0.1
0.0
ECMWF
3hr
6hr
ADV

32

SPRING:

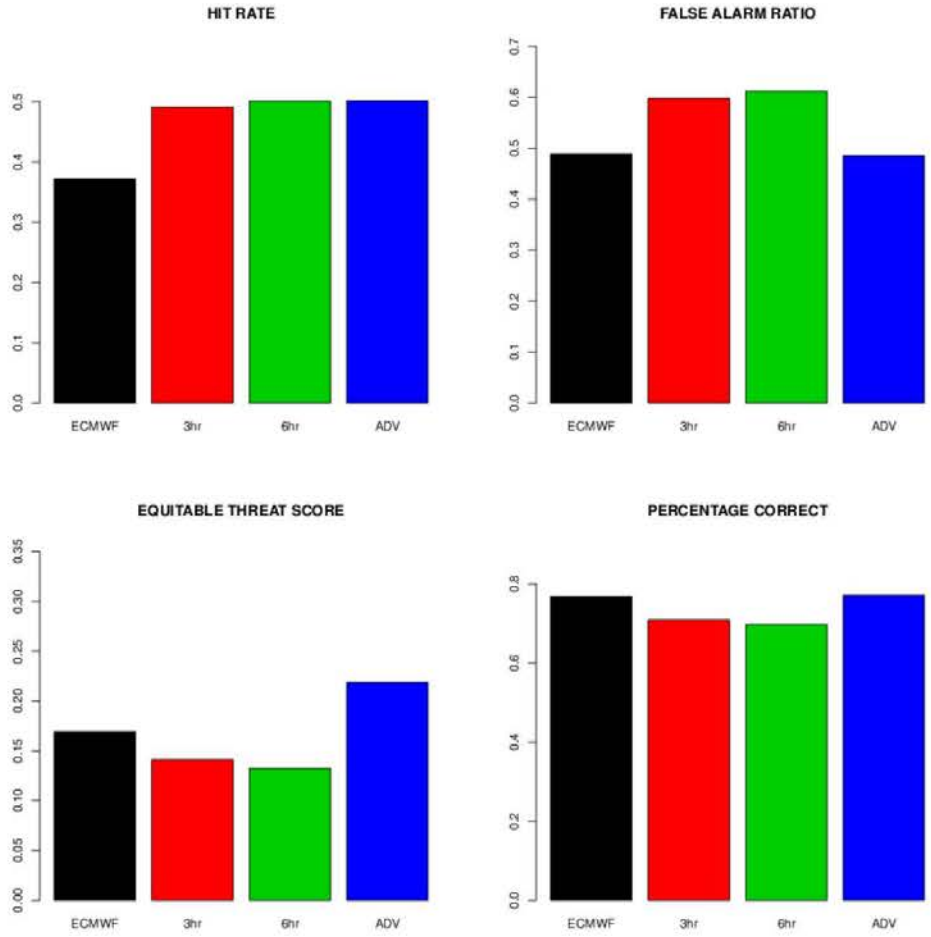

SPRING

33

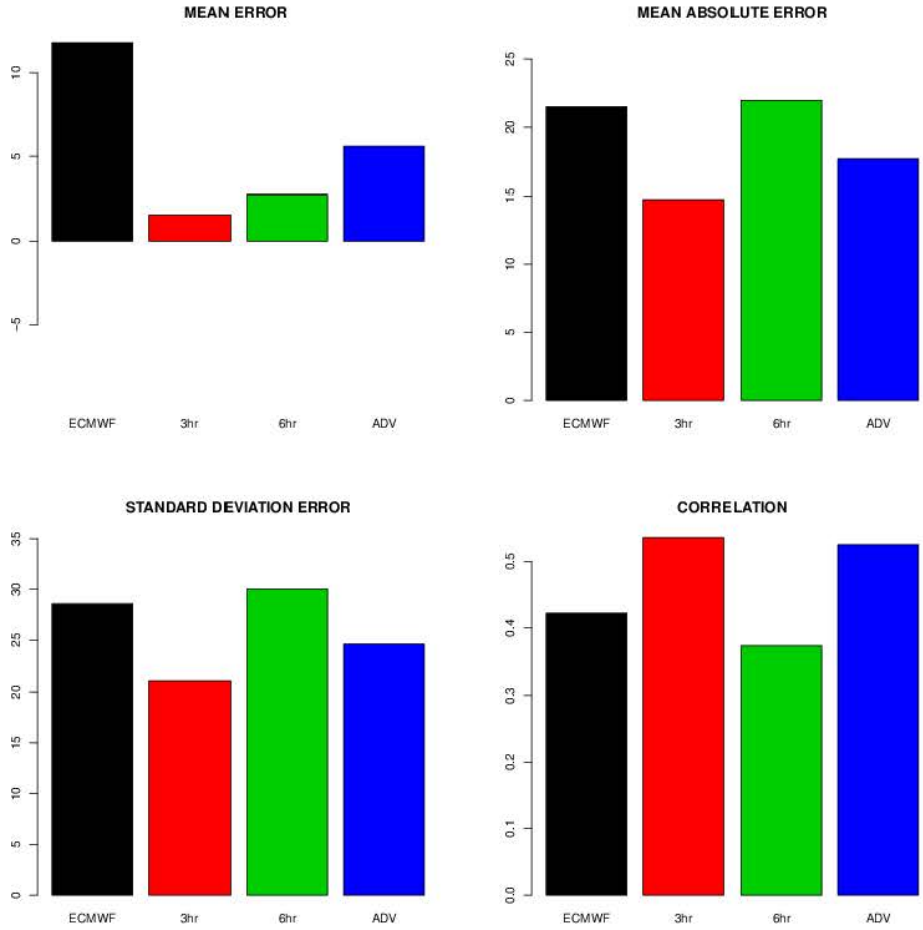
MEAN ERROR
10
5
0
−5
ECMWF
3hr
6hr
ADV
MEAN ABSOLUTE ERROR
25
20
15
10
5
0
ECMWF
3hr
6hr
ADV
STANDARD DEVIATION ERROR
35
30
25
20
15
10
5
0
ECMWF
3hr
6hr
ADV
CORRELATION
0.5
0.4
0.3
0.2
0.1
0.0
ECMWF
3hr
6hr
ADV

34

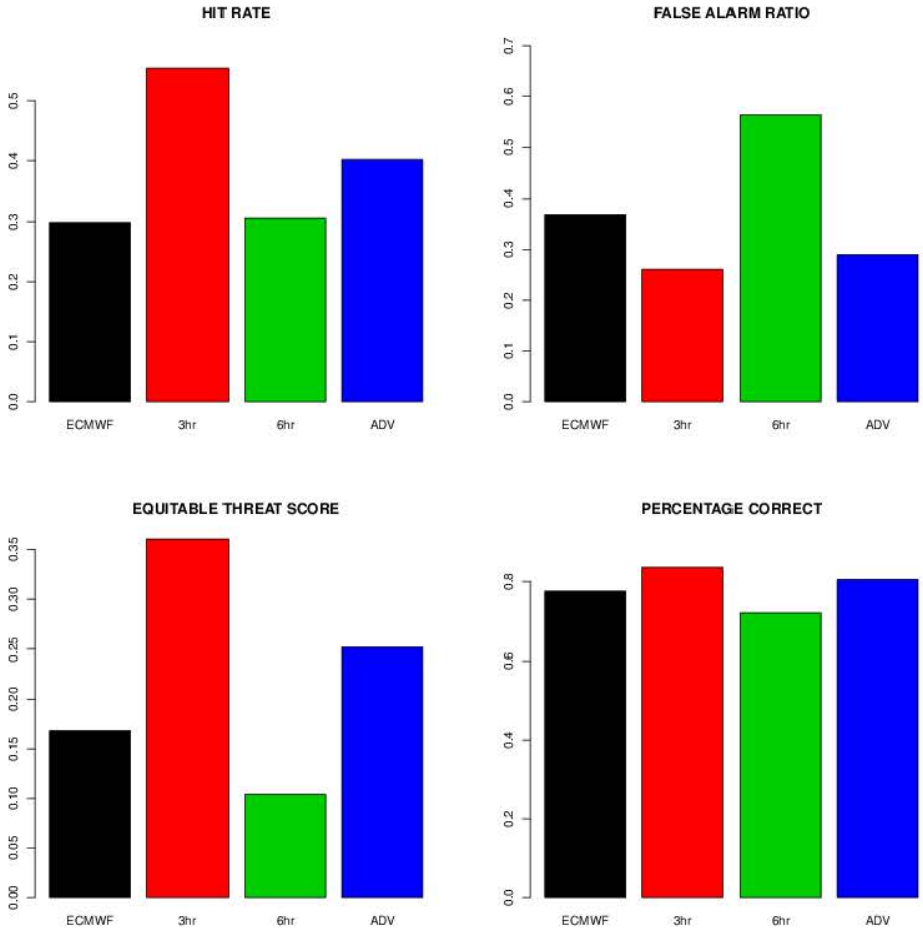
HIT RATE
0.0
0.1
0.2
0.3
0.4
0.5
ECMWF
3hr
6hr
ADV
FALSE ALARM RATIO
0.0
0.1
0.2
0.3
0.4
0.5
0.6
0.7
ECMWF
3hr
6hr
ADV
EQUITABLE THREAT SCORE
0.00
0.05
0.10
0.15
0.20
0.25
0.30
0.35
ECMWF
3hr
6hr
ADV
PERCENTAGE CORRECT
0.0
0.2
0.4
0.6
0.8
ECMWF
3hr
6hr
ADV

35

8 References

[1] "Description and verification of Cloud forecasts with short lead times in maritime areas.",
Morten Køtzow, Atle Macdonald Sørensen, Frank Tveter og Steinar Eastwood,
Meteorologisk institutt, 2015

[2] "Scientific and Validation Report for the Cloud Product Processors of the NWC/PPS",
NWC/CDOP2/PPS/SMHI/SCI/VR/Cloud, Issue 1, Rev.0d
27 june 2014